CHAPTER TWO

STRUCTURES LEFT BY MODERN MICROBIAL MATS IN THEIR HOST SEDIMENTS

Gisela Gerdes

INTRODUCTION

Microbial mats can generally be seen as "larger biofilms" (Costerton and Stoodley, 2003). Biofilms, i.e. closely related clusters of micro-organisms attached to a surface and often embedded in extracellular polymeric substances (EPS), embrace all metabolic pathways that ever emerged on Earth (Krumbein et al., 2003). Modern biofilm substrates are rock surfaces and deep cracks and fissures, soils, sedimentary granular systems of lacustrine, riverine and marine environments, and they occur from inside Antarctic ice to the walls of deep sea hydrothermal vents (Costerton and Stoodley, 2003). Biofilms are thus ubiquitous, microbial mats with the proviso that ecological conditions allow for the succession from biofilm to mat. Most successful in the enlargement of biofilms are cyanobacteria because of their great morphologic variability and biostabilisation capacity on sun-lit sedimentary surfaces. In combination with anoxygenic phototrophs, anaerobic and aerobic chemotrophs, organic and inorganic respiration and fermentation, cyanobacteria-dominated microbial mats successfully leave records in sediments, and thus, concomitantly and to a lesser degree, in the sedimentary rock record. Increasing interest in modern microbial mat features formed in siliciclastic sediments is complemented by a growing body of sedimentary features that are being found in Precambrian clastic sedimentary rocks, pointing to the important impact of such mats during Earth's earlier sedimentation record.

Generally speaking, microbial mats and their initial biofilms *per se* are relatively uncharacteristic in terms of facies, although shallow water and tidal environments composed of siliciclastic sediments host microbial mats across a broad spectrum of successional stages from cryptic biofilms to prolific mats, the latter being able to overgrow bedding planes by thicknesses of several centimetres. Yet, mat structures may appear also in lacustrine, riverine and other settings (Table 2-1), as do biofilms; they are even known from the oldest palaeo-deserts on Earth, ca. 1.8 Ga as will be shown in this volume.

Undoubtedly important within a facies framework are structures left by mat-forming micro-organisms when interacting with physical conditions of the depositional environment. A facies criterion in this respect is the time span available to create topographically heterogeneous laminae which may help to identify sedentary organic layers. From artificial mat cultivations, it has become known that a transition from a thin and fragile biofilm to condensed fibrillar meshworks of mat consistency needs several weeks of non-burial (Gerdes and Klenke, 2003). Lee-side shallow water environments of unusual salinity, rarely disturbed by sedimentation, are particularly successful in bringing out living three-dimensional surface layers. The term "living surface" illustrates well all dynamic processes constantly at work in mats: cell growth/replication, EPS production, motility/immotility, aggregation/dispersal etc.

In: *Atlas of microbial mat features preserved within the clastic rock record*, Schieber, J., Bose, P.K., Eriksson, P.G., Banerjee, S., Sarkar, S., Altermann, W., and Catuneau, O., (Eds.), Elsevier, p. 5-38. (2007)

During life, such dynamic systems overprint sedimentary surfaces, and after burial may leave behind uneven lamination which, in rocks, may provide a proxy for sedentary microbial life rather than for transported organic matter.

ORGANISATION OF PHOTOGRAPHIC MATERIAL

The photographic presentation of the following series of mat-related sedimentary structures is based on Schieber's (2004) process-related classification scheme, subdividing features according to (i) growth, (ii) metabolism, (iii) physical destruction and (iv) decay. This scheme is adopted as a framework throughout this book, and is discussed in detail in the next chapter.

Growth-related features and structures

Structures and fabrics related to the abundance and interaction of the main morphotypes (cyanobacterial filaments and unicells):

Figure 2-1-1: Biolaminites (single layer view);
Figure 2-1-2: Growth bedding;
Figure 2-1-3: Jelly forms, nodules, biscuits.

Structures generated from a change in growth direction

Figure 2-1-4: Pinnacles, tufts, microstromatolites;
Figure 2-1-5: Reticulate surface patterns;
Figure 2-1-6: Polygonal bulges, convoluted structures.

Features and fabrics related to trapping and binding of sediment

Figure 2-1-7: Microbial binding structures.

Microbial overprints of physically preformed bedding planes

Figure 2-1-8: Overgrowth, fixation and nivellement of ripples.

Features derived from metabolic effects

Figure 2-2-1: Mat-confined bubbles;
Figure 2-2-2: Layered iron enrichment;
Figure 2-2-3: Patterns resembling *Kinneyia*.

Features derived from physical mat destruction

Figure 2-3-1: Shrinkage cracks;
Figure 2-3-2: Jelly rolls, flip-overs;
Figure 2-3-3: Erosional edges, mat chips;
Figure 2-3-4: Ripple patches, *Astropolithon*-like features (sand volcanoes).

Features derived from mat decay and post-burial effects

Figure 2-4-1: *In situ* calcium carbonate precipitates in evaporite microbial mats;
Figure 2-4-2: Fenestral fabrics;

In: *Atlas of microbial mat features preserved within the clastic rock record*, Schieber, J., Bose, P.K., Eriksson, P.G., Banerjee, S., Sarkar, S., Altermann, W., and Catuneau, O., (Eds.), Elsevier, p. 5-38. (2007)

Figure 2-4-3: Gas domes;
Figure 2-4-4: Petee variations.

Structures owing their patterns to microbial growth (Figures 2-1-1 to 2-1-8) are closely related to the five subdivisions in the alternative classification scheme of "microbially induced sedimentary structures" (MISS), proposed by Noffke et al. (2001), and reflecting: (i) biostabilisation, (ii) levelling, (iii) baffling, trapping and binding, (iv) imprinting, (v) microbial grain separation (see also Chapter 3). Structures owing their patterns to mat metabolism (Figures 2-2-1 to 2-2-3) also relate to biostabilisation phenomena of sedimentary surfaces. Biostabilisation is also an important factor to explain structures owing their patterns to physical mat destruction (Figures 2-3-1 to 2-3-4). Finally the mat-related structures owing their patterns to the interplay of mat growth and mat decay in the subground are closely related to the biostabilisation potential of surface mats, as can be seen particularly in Figures 2-4-2, 2-4-3 and 2-4-4.

TERMINOLOGY

As is the case in many scientific fields, a plethora of terminology for microbial mats and their related features has emerged over the past several decades (see more discussion in Chapter 6 (c)). Many terms reflect similar features. Hofmann (2000) used the term stromatolite for "all morphologically circumscribed accretionary growth structures with primary lamination that is, or may be, biogenic". Krumbein (1983) suggested the term "potential stromatolite" if structures are modern. Burne and Moore (1987) related the term "microbialite" to both laminated and unlaminated accumulations of microbial origin. Earlier terms like "cryptalgal fabrics" (Aitken, 1967), "algal mats", "algal skin" or "algal carpet" (Black, 1933; Walter, 1976) have largely fallen away since the group of so-called "blue-green "algae" has been revised taxonomically into gram-negatively reacting photosynthetic cyanobacteria.

For tufts and pinnacles (Figure 2-1-4), the terms microstromatolite or microdome were also used. Reticulate ornaments, shown in Figure 2-1-5 and observed on various other mat surfaces, may give rise to wrinkle structures. Yet, there is no unifying use of this term. Hagadorn and Bottjer (1999) assume that wrinkle structures may occur in various modifications in the presence of microbial growth. Noffke et al. (2002, 2003b) interpreted fossil wrinkle marks to represent load marks of buried mats. Abiotic genesis of "*Runzelmarken*" was experimentally studied by Reineck (1969). Sarkar et al. (2004) argued that wrinkle structures observed in certain Precambrian sandstones developed due to sand flow around synaeresis cracks protected by a mat. The complexity of wrinkle marks and their possible genetic influences will be explored in Chapter 6(a).

Bulges and involute structures (Figure 2-1-6) are also termed "compression double bulges" by Noffke (2000). Ripple overprints (Figure 2-1-8) may also generate "palimpsest ripples" (Schieber, 2004, his Fig. 7.9-1a). Shrinkage cracks (Figure 2-3-1) are also named desiccation cracks, sun cracks (Fischer, 1964, p. 114; cited in Fagerstrom, 1967), or contraction cracks (Fairbridge and Bourgeois, 1978). Other terms for mat chips (Figure 2-3-3) are microbial sand chips, organosedimentary fragments, or eroded mat fragments. Ripple patches (Figure 2-3-4) are also termed erosion pockets (Gerdes et al., 1993). *In situ* carbonate precipitates in microbial mats (Figure 2-4-1) are summarised under the term "biominerals" (Flügel, 2004). Another term for fenestral fabrics (Figure 2-4-2) is "sponge pore sand" (Noffke et al., 1997b; ancient analogues: Noffke et al., 2003b). Flügel (2004) refers to laminoid fenestral fabrics.

ENVIRONMENTAL ASSOCIATIONS

Microbial mat-related structures and features in this chapter are from modern transitional areas between land and sea (Table 2-1). Considering the settings according to their degree of exposure, the sequence follows from permanently water-filled shallow lagoons, transitional areas between lagoon and adjacent areas, intertidal flats, intertidal-supratidal transitions and finally supratidal flats and sabkhas (Table 2-1). Sediments bearing these structures and features are partly pure siliciclastic (e.g., Figure 2-1-1), or siliciclastics mixed with evaporites (Figure 2-1-3 F), detrital carbonate grains (Figure 2-1-2 H), or *in situ* carbonates (Figure 2-4-1).

Krumbein et al. (2003) argued that microbial mats and their products may occur "at any place offering biologically available water and temperatures… which comprises the whole geomorphologic range from approximately 10 km above to 10 km below NN… ". Yet modern planar forms as presented in this contribution are prevalent at low energy levels (Sami and James, 1993; Schieber, 2004). Further, experience with modern microbial mats from settings indicated in Table 2-1 suggests that photoautotrophic biofilms following a succession towards thick mature microbial mats need sufficient time spans of non-burial. Transient biofilms can form rapidly (within 20 minutes) and usually disperse shortly before or after the tidal exposure period ends (Paterson et al., 1998, 2003). Yet, thick multi-laminated surface carpets need time spans of several weeks, if not of several months (Gerdes and Klenke, 2003) of exposure. Thus, on closer examination of fossil microbial carpets on bedding surfaces it would be worth thinking about the kind of environment which could have ensured longer time spans of non-burial.

Several sedimentary structures grouped in Table 2-1 may occur also in a variety of other settings, including subaqueous marine and non-marine facies, since mat-forming cyanobacteria are not by any means restricted to peritidal settings. Particularly, structures related to metabolic activity (Figures 2-2-1 to 2-2-3) or post-burial decay of mats (Figures 2-4-1 to 2-4-4) may occur in subaqueous environments. Even cracks and incomplete polygons may be subaqueous phenomena (Donovan and Foster, 1972), although facies relationships have been a matter of debate (Astin and Rogers, 1991, 1993; Barclay et al., 1993). Fossil roll-up structures were described from shelf deposits below wave base (Simonson and Carney, 1999), although the authors assume that the microbial mats involved may not have been based on photosynthesis. These authors apply the term roll-up structures to features from depositional environments below wave base, and refer to "jelly rolls" if peritidal shallow-water features are described (such as in Figure 2-3-2). Source areas of mat chips may be shallow peritidal lakes, lagoons and their adjacent flats (Figure 2-3-3); on the other hand, accumulation areas may be subaqueous (Schieber, 1999, his Fig. 12H). Photosynthetically produced oxygen bubbles may cause flotation of thin, loosely attached crusts (Fagerstrom, 1967; a similar example is illustrated in Figure 2-3-2 G). According to Flügel (2004), aligned fenestral cavities caused by the interplay of post-burial processes and sealing effects of mats (Figure 2-4-2) may develop in both subaqueous and subaerial settings, (as do cyanobacterial mats). Domes (Figure 2-4-3) may be characteristic of periodically subaerially exposed hypersaline lagoons; yet gas doming is not restricted to arid areas but occurs also on tidal flats of the temperate humid climate zone, as well as in various other environments. Theoretically, gas-doming may also occur subaquatically, although forming mainly under intertidal to lower supratidal conditions (Bouougri and Porada, 2002). To seal their surfaces well, thick cohesive mats may need repeated phases of submersion, e.g., in a seasonal cycle (Figure 2-4-3 G). Finally, *Kinneyia* may be subaqueous phenomena, although modern structures resembling

In: *Atlas of microbial mat features preserved within the clastic rock record*, Schieber, J., Bose, P.K., Eriksson, P.G., Banerjee, S., Sarkar, S., Altermann, W., and Catuneau, O., (Eds.), Elsevier, p. 5-38. (2007)

Kinneyia may occur on peritidal evaporative flats, where surface sediments are enriched in watery gels by dominance of coccoid cyanobacteria (Figures 2-1-6 and 2-2-3).

INFERRED SEDIMENTARY AND BIOLOGIC PROCESSES, IDEAS ON GENESIS

Sedimentary features and structures related to growth

Structures related to the local abundance of different morphotypes (Figures 2-1-1 to 2-1-3)
Sedimentary structures shown in this section relate to cell growth and replication, production of extracellular polymers (EPS), mat growth and layered biomass condensation in time and space. Most important are physio-ecological responses to physical triggers, e.g., light meeting a mat surface, depth of overstanding water and shading. Growth bedding of the biovarvite type (Figures 2-1-2D to 2-1-2G) is common in protected peritidal lagoons controlled by higher evaporation and salinity (Gerdes et al., 2000b). Seasonally changing water depths corresponding to fluctuations in light intensities trigger the stacked buildup of sets of dark/light laminae. The dark horizontal layers are products of local abundance of filamentous cyanobacteria. The often more extensive light layers are made of coccoid cyanobacteria, large amounts of protective EPS, and often are interspersed by authigenic mineral precipitates. Light surface laminae provide shading for low-light filaments which remain beneath the translucent mats in summer. In winter, filamentous species benefit from decreasing light intensities and a higher water level, and over-ride the coccoid mats. Thus, a seasonal rhythm is indicated by the sets of hydroplastic and filamentous layers (Gerdes et al., 1994b). Such slowly growing sequences store high amounts of organic matter and enhance upward movement of fronts of sulphate-reducing bacteria and H_2S.

On intertidal flats, high levels of light intensity meeting surface mats lead to a productivity increase some millimetres beneath sedimentary surfaces (Garcia-Pichel and Castenholz, 1994). However, as long as surface sediments are damp to ensure water availability necessary for life processes, growth bedding can also rise above subaerial surfaces. Repeated low-rate sedimentation serves as a trigger that forces buried filamentous cyanobacteria to move upwards and over-ride the new sediment surface, producing the type of growth bedding driven with the aid of mineral sedimentation (Figures 2-1-2A to 2-1-2C).

The relief cast in Figure 2-1-2C exemplifies how environment-specific frequency and rates of sedimentation can control the interposition of mats within a sedimentary sequence. In the lower part, two cross-stratified sediment layers, each separated by a monolayered microbial mat, represent storm sand layers which irreversibly buried underlying mats and left behind single biolaminites. A sequence of closely stacked mats in the middle part of the relief cast indicates calmer conditions associated with low-rate sedimentation. These common summer conditions induce the type of growth bedding modelled in the experimental build-up in Figure 2-1-2B.

Sufficient time for growth is an important factor influencing the characters of biolaminites as they appear in vertical sequences. Initial propagation of mat-forming organisms on a bedding surface, the essential construction zone of mat formation, often is not linear. To amalgamate into bundles and tangles (a prerequisite of mat formation), trichomes need time (Figure 2-1-1D). A coherent mat which homogeneously covers the substrate may need several weeks of almost zero deposition (Gerdes and Klenke, 2003).

Single buried mats of lower thickness within sedimentary sequences may indicate pioneer stages which, after short periods of non-deposition, became buried again (Figures 2-1-1A, B). Increasing biomass condensation, and the buildup of three-dimensional networks (biodyction; Krumbein et al., 2003) are hints on sediment starvation (Figure 2-1-1C).

Coccoidal surface populations are dominant components of hypersaline shallow water and dessication-endangered arid settings. The more physical harshness increases in these habitats, the more coccoids persist in increasing abundance. Large amounts of EPS, viscous polysaccharide solutions and protective pigmentation are attributes that allow for inhabiting environments of extreme light radiations (Figure 2-1-3). Also, processes of space competition may be facies-relevant (Figures 2-1-2D to 2-1-2H). The overriding phenomenon is well visualised in Figure 2-1-3A showing filamentous cyanobacteria in space competition with coccoids for the most optimal light position.

The dominance of coccoid cyanobacteria is often indicated by a characteristic irregular surface topography including mammillate, jelly, cushion-like or cauliflower-like patterns (Figure 2-1-3). Mammillate surface patterns may also originate from nodules in which unicellular cyanobacteria with multiple fission such as Pleurocapsalean taxa are involved (see intrasedimentary nodules in Figure 2-1-3C). Nodule formation may indicate changing levels of salinity and water cover (schizohaline conditions; Gerdes et al., 1985). Nodular salt crusts (Figure 2-1-3F) form on higher sabkha flats where microbial growth and slime production interfered with salt precipitation from hypersaline groundwater transported to the surface by evaporative pumping (Noffke et al., 2001). As is the case for quartz sands, gypsum crystals are ideal in light channelling.

Structures generated from a change in growth direction (Figures 2-1-4 to 2-1-6)
Filamentous cyanobacteria, which originally contribute to the basic mat, are able to change their growth direction into a vertical position and rise above the mat base. Results are tufts and cone-shaped pinnacles some millimetres high. When stabilised by EPS, initially soft and flexible tufts change into rigid pinnacles. Different filamentous species are able to initiate pinnacle formation. Examples are *Microcoleus chthonoplastes* (Figure 2-1-4A, 2-1-4C to 2-1-4F), and *Lyngbya aestuarii* (Figure 2-1-4B, 2-1-4G to 2-1-4H). The knotty structures result from a combination of growth and movement of filaments in response to environmental factors such as light, ionic composition of interstitial and surface water, or oxygen supply. The outer form and size depends largely on the presence of the respective species morphotype. Raised tufts and pinnacles formed by *M. chthonoplastes* are usually smaller than of *Lyngbya* ssp. The knotty surface structures of *L. aestuarii* in Figure 2-1-4G and 2-1-4H protrude up to 20 mm out of the sediment. They resemble structures at Shark Bay made by the same species, forming radiating bunchlets (Golubic, 1976). Such relatively permanent structures may also benefit from the participation of other filamentous genera, e.g., *Schizothrix* (Golubic, 1992).

Distribution patterns of pinnacles (Figure 2-1-4D to 2-1-4F, see also Figure 2-3-1H) seem not to be random, but may reflect oriented behaviour probably triggered by small-scale differences in nutrient concentrations, shading, or even space competition. The curious concentric arrangement of pinnacles in the so-called “fairy rings” (Figure 2-1-4F) may be a sign of oriented behaviour of pinnacle-forming organisms. Although no sufficient explanation exists until now, one idea was that concentric micro-waves initiated by gas bubbling through small exit points within mat surfaces propagate nutrient fronts which may trigger chemotactic responses (Gerdes et al., 1994a).

Pinnacles combined with reticulated patterns are shown in Figures 2-1-5A to 2-1-5C. Particularly thick elongated bulges are shaped by dominance of *Lyngbya aestuari* (Figure 2-1-5D). Browne et al. (2000) describe similar reticulate mats from Shark Bay composed of ridges dominated by *Lyngbya* sp. These authors assume that filaments have greater advantage of upwards growth and thickening of bulges where O_2 is more available. In Figure 2-1-5A, distinct microbial populations contribute to individual parts of the surface texture (Gerdes and Klenke, 2003): green reticulate strips and pinnacles can be traced back to *M. chthonoplastes*, species of *Spirulina* are abundant within yellow brown strips and pinnacles, and coccoids (e.g., *Synechococcus* sp.) form the yellow cushions in between.

Macroscopically, the reticulate patterns resemble "elephant skin" (Figure 2-1-5E; Gehling, 1991). Striking similarity exists between these patterns and wrinkle structures described by Hagadorn and Bottjer (1997). The studies illustrated in Figure 2-1-5 confirm the suggestion of Gehling (1999) that reticulate mat textures are characteristic of thick (mature) microbial mats. Experiments using lab-cultured mats have shown that the development of a reticulated mat texture necessitates time spans in the range of several months when mats are not disturbed by burial (Gerdes and Klenke, 2003). Knowledge of the tendency of filamentous cyanobacteria to amalgamate into bundles and tangles, to change their growth direction and to produce non-linear growth patterns may help to explain often topographically heterogeneous bounding planes in internal sequences (Fig. 2-1-5F).

Involute structures (Figure 2-1-6) may be products of complex interconnected processes which include tactic responses of mat-forming cyanobacteria to surface cracking, increasingly confined space and self-shading due to continual growth (Noffke, 2000). Multilayered crack tapestries may indicate repeated wetting which supplies the micro-organisms with essential water (Figure 2-1-6B). Mats finally protruding above the filled cracks form bulges which mark the former polygonal crack patterns (Figures 2-1-6D to 2-1-6F).

Features and fabrics related to trapping and binding of sediment (Figure 2-1-7) In life, erect cyanobacterial tufts function as binders and bafflers, providing a trap for sediments, organic debris or calcium carbonate precipitates in the water column (Figure 2-1-7A). Of sedimentological importance is the "fly paper effect" of sticky mat surfaces which provide traps for detrital grains. Grains providing favourable solids are bound by filaments and thick filament clusters and incorporated into the microbial laminae. Grains trapped and bound by microbial mats aid the upward-directed growth of multilaminated mat sequences (Figure 2-1-7B).The reduction of mechanical friction within the soft matrix surrounding the quartz grains aids the rotation of the grains to an energetically suitable position, resulting in grains orientated with their long axes parallel to the biolaminite (Figure 2-1-7E). In closely packed sediments, gravity-related orientation is not possible (Noffke et al., 1997a). Another effect of trapping and binding is the selection of heavy mineral grains by microbial mat surfaces (Figures 2-1-1B, 2-1-7F).

Ripple overgrowth and nivellement (Figure 2-1-8) In open intertidal flats or beaches, surficial biofilms may relatively rapidly overgrow rippled surfaces during stages of sediment starvation. Preferred sites for initial growth are leeward faces of ripples (Figure 2-1-8A,B). Such biofilms are not coherent enough to modify the primary physical structures, although stabilisation effects may be possible. At topographically higher or more protected sites, mats are able to increase their surface-modifying productivity. This is depicted in the sequence of

photographs in Figures 2-1-8A to 2-1-8F, from thin initial biofilms to the increase of surficial biomass and finally completely overprinted ripple marks.

Microbial effects (biostabilisation, trapping, binding sediments) interfering with mechanical reworking are able to produce chaotic ripple patterns (Noffke, 1998). Sinoidal structures evolving from microbial drapes of ripple troughs and leeward faces are described by Noffke et al. (1997b). Ripple levelling proceeds during longer-lasting periods of non-deposition or non-erosion, in which the mats have the possibility to overprint the surface with thick condensed biomass. Baffling/binding may be a favourable process for ripple levelling (Noffke et al., 2003a).

Features derived from metabolic effects

Closely linked metabolic and decay processes (Figure 2-2-1) Well developed, highly diverse microbial mats represent ecosystems in which both the upward directed primary growth and the degradation of the organic matter are closely linked via biochemicals which are excreted by the one group, used and transformed by the other (Stal, 1994). In dealing with product-process relationships, it is thus not easy to make a clear separation between features/structures related to metabolic effects, and those related to mat decay. An example is the precipitation of calcium carbonate in microbial mats which may be seen in relation to cyanobacterial taxa controlling calcification processes directly (Merz, 1992), or in relation to autotrophic CO_2 depletion, or to heterotrophic pathways in which numerous bacterial groups through degradation of the organic substrates passively create the chemical milieu for carbonate precipitation (Castanier et al., 2000; Schneider and Le Campion-Alsumard, 1999). Friedman et al. (1992) stated that a sedimentary product "itself might not convey information pointing to a single specific process". This should be kept in mind when looking only for a single explanation of structures, such as the bubbles shown in Figure 2-2-1, but almost also throughout the other figures shown in this contribution.

Bubbles may be encountered with various metabolic activities. Processes concerning carbon and sulphur metabolism take place even in the topmost few millimetres of mats, photosynthesis occurring simultaneously with respiratory reactions. Sulphate reduction occurs at high rates in close proximity to, or even within, the phototrophic zone of microbial mats (Skyring et al., 1989). Even oxygen and hydrogen sulphide can coexist in high concentrations for extended periods of time, probably caused by the low diffusivity of gases through cyanobacterial slimes (Krumbein et al., 1979). Bubbles resulting from the activity of various physiologic groups may thus contain O_2, CO_2, H_2S or CH_4.

In shallow water environments, photic conditions are also modified by diffusion processes across the sediment-water interface making the overstanding water viscous and "sticky" (Jorgensen, 1994). Slime-captured bubbles, threads and flocs contribute to shading which may support pelagic propagation of biofilms above the benthic mats (Figures 2-2-1A to 2-2-1E).The heterogeneous three-dimensional structures may contribute to topographically heterogeneous microbial laminae within internal sediments.

Subaerially exposed surfaces generate bubbles if surface sediments are sludgy from microbial slimes which slow down diffusion of gases. Sludgy sediments or gypsum mush glued together by microbial slimes also capture bubbles giving rise to blistered sedimentary surfaces (Figure 2-2-1F). Sulphate nodules embedded in microbial mats may result from metabolic activity of

chemolithotrophs or sulphur bacteria (Figure 2-2-1I). Internal bubbles may also provide nuclei for carbonate precipitation.

Iron precipitation in mats (Figure 2-2-2) Black iron sulphide deposits are particularly significant in coastal microbial mats in which sulphate-reducing bacteria are active (Figure 2-2-2H). Cores taken from microbial sediments usually show the dark colours of reduction almost up to the surface, eventually topped by red and green zones indicating anoxygenic and oxygenic photosynthesis. Immediately below mats dominated by *Microcoleus chthonoplastes*, sharp layers of iron hydroxides are sometimes obvious (Figure 2-2-2A, see also Figure 2-1-7B). According to Stal (1994), *M. chthonoplastes* is capable of binding iron to the polysaccharide sheaths where the iron is reduced concomitant with its binding. This same author reports advantages of this process for the organisms: (i) binding and reduction of iron makes this element available for metabolic processes; (ii) since ferrous iron reacts rapidly with oxygen, the accumulation of ferrous iron in the immediate vicinity of the cell may keep oxygen partial pressure low. This enhances the efficiency of CO_2 fixation and limits photorespiration; (iii) in the view of community metabolism, ferric hydroxides underneath the cyanobacterial layer may function as barriers protecting the overlying cyanobacteria from sulphide which is produced in the deeper anoxic layers, as well as preventing oxygen from reaching the anaerobic microbial community.

Physio-ecologic processes in mats certainly interact with physico-chemical dynamics proceeding across sharp redox gradients which are characteristic of multilayered microbial mats. Schneider and Herrmann (1980) developed the model of iron mobilization from underlying anoxic layers giving rise to sharp layers of iron hydroxides below photosynthetic active mats (Figures 2-2-2F to 2-2-2G). Evaporation pumping may support upwards-directed pore water flows, whereas strongly entangled meshworks dominated by *M. chthonoplastes* or similar morphotypes may slow-down the pore water flow so that iron hydroxide can precipitate below.

Finally it should be noted that rusty-brown iron hydroxide horizons may also develop after cross-cutting of fresh material which opens oxygen windows. The ferrous iron enriched in buried microbial mats reacts soon with the oxygen. Therefore, it cannot be excluded that the rusty-brown iron hydroxide horizons in Figures 2-2-2B, 2-2-2D and 2-2-2E might be preparative artefacts.

Sulphate-reduction starts immediately within decaying mats giving rise to lamina-specific pyrite arrangements (Figures 2-2-2B and 2-2-2C). Also, ferric iron reacting with sulphide may result in the formation of stable pyrite (Stal, 1994).

Wind-derived ripples in microbial slime-sediment sludge (Figure 2-2-3) Ripples are characteristic features of sabkha sediments agglutinated by microbial slimes and precipitating salts. The structures in Figure 2-2-3 were observed on higher-lying parts of coastal sabkhas where coccoid cyanobacteria (*Aphanocapsa* sp., *Gloeothece* sp.) dominated the surface mats. Gavish et al. (1985) described hollow ripple structures folded like table cloths by wind. Locally also, subsidence of the slushy sediment down a gentle slope may produce similar folds. Photosynthetic gas bubbles captured in the slime are aligned by the ripples. Gas from decay also may be involved since decay may start already within the uppermost centimetres of a mat (Stal, 1994). Pflüger (1999) mentioned that "*Kinneyia"* style ripples may reflect gas trapping beneath flat mats. Yet the aligned bubbles in Figure 2-2-3 mark ripple crests, while Pflüger (1999) indicates that trapped bubbles correspond to the troughs of "*Kinneyia*".

Features derived from physical mat destruction

Presence of mats change the rules (Figure 2-3-1)…. The rule that cracks do not form in pure sand does not hold true where microbial mats are abundant. Thus, fossil records of shrunken sand layers must have had an additional component that could shrink during dehydration, a microbial substrate being the most likely candidate (Schieber, 2004). Also, the rule that large cracks develop in thick and smaller cracks in thin surface beds does not hold true where microbial mats are abundant. Thin microbial mats are able to produce extraordinarily wide cracks (Figures 2-3-1A to 2-3-1E).

The presence of a mat may be indicated by multiple incomplete sub-fracturing of crack margins, imparting cauliflower-like patterns (Figure 2-3-1D). The fibrillar network of filamentous cyanobacteria controls irregular and incomplete sub-fracturing, giving rise to blotting paper effects (Gerdes et al., 1993). Viscous microbial mats experience particularly high reduction of surface volume owing to dehydration or desiccation (Figure 2-3-1E, see also Figures 2-4-4B, 2-4-4C).

Slippery sediments effectively prevent attachment. Mats easily scour and tear, or are moved due to wind or water stress. In quartz sand, on the other hand, characteristic biodyctions develop (Figure 2-1-1C) which effectively intertwine with the sand grains and are far less removable than mats on slippery clay (Figure 2-4-4B) or evaporites (Figure 2-3-1E, see also Figures 2-3-2E to 2-3-2G and Figure 2-4-4C).

The bottom of an abandond salina basin shows well the difference between crack morphologies in clay and microbial mats. In the underlying clay, cracks are orthogonal, while volume reduction in the elastic surface mat has left behind irregular and partly incomplete polygons showing folds and upcurled margins (Figure 2-3-1I).

In higher parts of a supratidal setting, unusual crack morphologies have been observed supported by the flexible behaviour of surface sediments made viscous and sticky by microbial slimes (Figures 2-3-1F, 2-3-1G), see also Figures 2-3-2A, 2-3-2B). Mats naturally include various defects and local thickness variations which may also explain unusual rupturing. Also, healed-up former cracks provide such local unevenness (Figure 2-3-2A).

Specific milieu conditions within the cracks attract organisms from adjacent mats to invade the cracks where they benefit from damp conditions and additional space for attachment. Results are rounded edges and pillow structures (Figure 2-1-6).

Desiccation and curling-up edges of cracks, jelly rolls (Figure 2-3-2) Figure 2-3-2 reflects the cohesive behaviour of soft and jelly-like surfaces of microbial origin. Schieber (1999) emphasize the flexible behaviour of soft mats when rolled up and transported by currents. Such overfolded rolled up fragments also help to distinguish cohesion due to microbial binding from cohesion caused by synsedimentary cementation (Schieber, 1999). The patterns in Figure 2-3-2 may belong to a similar category of features known as “jelly-roll” structures, which have been described from Phanerozoic carbonates (Demicco and Hardie, 1994, cited in Simonson and Carney, 1999).

Variety of conditions involved in chip production (Figure 2-3-3) Cohesiveness of advanced stages of microbial mats is particularly obvious at erosional edges (Figure 2-3-3).

Margins undermined by currents tear and become fringed (Figures 2-3-3A to 2-3-3C). Such conditions, but also mat cracking (Figure 2-3-1), jelly rolls (Figure 2-3-2) or gas from the subsoil may give rise to the genesis of mat chips. Chip characters depend on (i) mat types, (ii) substrate types, (iii) forces which release the chips, (iv) source area, (v) depositional areas. Main mat types as presented here include fibrillar microbial meshworks strongly entangled with the subsediment (Figure 2-1-1C), or loose, often monolayered mats enriched in hydroplastic gel (Figure 2-3-2). During decay, single-layered, often scummy mats get peeled-off piece by piece from the substrate, by moving water. The substrate determines the efficiency of entanglement of biofilm organisms with the subsoil. Entanglement seems to be less effective in clay or slippery gypsum mush (Figure 2-3-2). Forces which release mats from the subground include erosion by currents or wind, desiccation and subsequent erosion, or gas pressing from below on to the surface mats. Source areas of chips can be various (as are formational sites of cyanobacterial mats). Finally depositional areas of chips may be far away from source areas, e.g., towards deep subtidal zones. Particularly flake-like chips are easily transported. Wind transport of dry chips also provides "meteor paper" (Krumbein et al., 2003).

Erosive forces acting upon biostabilized sediment surfaces (Figure 2-3-4) Ripple patches in microbial mat-stabilized sand flats (Figure 2-3-4A) are caused by tide-controlled waves and currents which act upon the sedimentary surface. Although microbial films and mats attenuate the effects of erosive forces, the protective biofilm may be locally destroyed where obstacles (e.g., skeletal hard parts) lying in the path of currents, or storm surges cause vortices and small-scale rip currents (Gerdes et al., 1993; Noffke, 1999). Where microbial binding is lacking, the unsecured sand becomes rippled. Ancient examples have been reported from the Cretaceous Dakota Sandstone (Reineck, 1979) and from various units in the Belt Supergroup (Schieber, 1998). The shape of such ripple patches is strikingly different from obstacle marks, which occur in sediments lacking biofilms or mats. The features can not readily be confused with weathering of a fossil bedding plane through which a lower rippled layer is laid free (Schieber, 1999). In case of such "windows", there will be a sharp break between the rippled subground and the remaining cover. In contrast, ripple patches evolving from partial mat erosion exhibit smooth transitions between the ripples and the margins of the remaining surface mat (Figure 2-3-4B).

Sediment volcanoes ("*Astropolithon*"; Dawson, 1878) are associated with the expulsion of water from sediment as a result of slumping, very rapid sedimentation, or agitation of freshly deposited sediment (Reineck & Singh, 1980). According to Pflüger (1999) and Seilacher and Goldring (1996), such structures can only form in cohesive host sediment, e.g., microbially bound sand (Figures 2-3-4C, 2-3-4D).

Features derived from mat decay and post-burial effects

In-situ carbonates (Figure 2-4-1) Against the background of the introductory remarks in this chapter, it seems acceptable to subsume carbonate precipitates in Figure 2-4-1 under features derived from mat decay and post-burial effects. Genesis, form, size and arrangement of carbonate precipitates are strongly influenced by the members of the mat community and internal heterogeneous micro-textures. Various studies have associated *in situ* calcium carbonate precipitation in mats with degradation of biomass in zones containing purple bacteria and heterotrophic bacteria (Kühl et al., 2003, for discussion). The distribution of precipitates seems not to be random, and features evolving from microbial coating of mineral particles indicate active growth response of microbial inhabitants to interfaces (Gerdes et al.,

1994a). Granular carbonates in plastic gel (Figure 2-4-1D) form around nuclei which may have been cells or cell clusters, liquid or gaseous bubbles, or tissue remains of mats. Growth-bedding confines particles into a layered appearance (Figure 2-4-1A). Different particle types coexist in microbial mats, including peloids, ooids or botryoidal lumps (Figures 2-4-1 B to 2-4-1F). The term "sedimentary augen structure" (Dahanayake et al., 1985) denotes fabrics owing their structures to interaction of particle growth and elastic response of filamentous mats (Figure 2-4-1D). Ooids are common where individual nucleation centres are isolated in the viscous gel or between filamentous laminae. Metabolic vesicles or bubbles may also provide adequate interfaces for bacterial attachment and subsequent carbonate precipitation (Figure 2-4-1E). Botryoidal forms (Figure 2-4-1F) reflect amalgamation of carbonate precipitates in close proximity surrounded by microbially active biogenic substrates. Over-riding processes triggered by seasonal cycles of environmental variables are recorded in the vertical section in Figure 2-4-1G). The vertically to diagonally oriented filaments demonstrate active movements of filamentous cyanobacteria, encrustation in life position and death with progressing mineralization.

In-situ carbonate precipitates of biogeochemical origin usually reveal heterogeneous distribution patterns within the mat fabrics (Figures 2-4-1A to 2-4-1G). On the other hand, inorganic carbonate crystallization from brines is also possible (Schneider and Herrmann, 1980). Results are homogeneous white layers covering the mat surfaces as indicated in Figure 2-2-2F to 2-2-2H).

Surface sealing by mats interacting with post-burial gas production (Figure 2-4-2 and 2-4-3) Fenestral fabrics (Figure 2-4-2) are closely related to the deformation of primary fabrics and cohesive bedding planes owing to the pressure of gas released from deeper buried organic matter. Gas pressure greater than the resistance of the sediment grains results in the formation of secondary voids (Noffke et al., 1997b). Fenestrae arranged concordant to biolaminites (Figures 2-4-2A, 2-4-2C, 2-4-2D) are a consequence of the sealing effect of buried mats connected with compaction of subspherical gas bubbles (Flügel, 2004). Interactive gas pressure from decaying organic material and surface sealing by mats cause also lifting and separation of mat surfaces from the adjacent sediment (Figure 2-4-2E and Figure 2-2-2F; Logan et al., 1974).

In Figure 2-4-3, mats are flooded and non-mineralised prior to and during deformation due to gas pressure. Gas diffuses from deeper buried organic deposits or mats toward the surface where cohesive microbial tissues retard the exchange through the mat-water interface. Hummocks may rise up convexly over selective vents (Figures 2-4-3A to 2-4-3D). Subaerial exposure supports gypsum and halite encrustation, possibly also forced by evaporative pumping (Figures 2-4-3D to 2-4-3H). If domes do not experience salt encrustation, continuous gas concentration beneath the surface mat may increase the tension along weak zones, establishing circular cracks at transitions from the planar to the domed mat (Figure 2-4-3B).

Well-known "cabbage-head" structures (Figure 2-4-3G) are products of intermittent flooding associated with domal mat overgrowth, and subaerial exposure associated with mineral encrustations.

"Petee"-variations (Figure 2-4-4) Reineck et al. (1990) subsumed domes, folds and their transitions (Figure 2-4-4A) under the term "petee" and defined petees as overthrust structures in biogenic matrix. Initially, the term "petee" was created by Gavish et al. (1985) to contrast

biogenically rounded positive structures (petees) from abiogenic sharp-edged triangular “tepees”. Reineck et al. (1990) termed domes and folds in soft mats ‘alpha-petees’and related these structures to subsurficial gas pressure caused by post-burial decay of buried mats. These authors termed gypsum-encrusted stages of initially soft-ground domes and folds in arid climates ‘beta-petees’ and related these still to post-burial decay and gas production of buried mats (Figures 2-4-4A, 2-4-4B). Circular tearing of soft monolayered mats and circular subsoil exposure may form due to particularly stron g gas pressure from below (Figure 2-4-4B). Repeated changes between wetting and exposure favour the formation of massive gypsum. Wetting encourages populations of microbial coccoids to colonise outer petee surfaces. Tan colour in Figures 2-4-4D and 2-4-4E indicates slime coatings produced by numerous coccoid cyanobacteria whichprotect themselves against phototoxic reactions by carotenoids and EPS.

However, folding supported by wind and water friction (Figure 2-4-4C), and expansion of gypsum-encrusted surface mats also produce overthrust structures. Reineck et al. (1990) termed the latter ‘gamma-petees’ (Figure 4-4 F) and defined them as intermediates between petees and tepees due to the same underlying process. Expansion of surface crustsmay also cause cracking and subsequent movement of the cracked crusts against each other (Figure 2-4-4F). In vertical section these structures show the characteristic tent (tepee) form (Assereto and Kendall, 1977; Reineck et al., 1990). Gamma petees evolve from the same processes, but in the presence of biogenic matrices which smooth sharp edged overthrust structures. Tepee and gamma petee structures may be characteristic of higher-lying sabkha flats (Figure 2-4-4G).

Table 2-1.
Environmental settings for structures and features illustrated in this chapter

Environmental settings
Temperate-humid tidal flats of Mellum Island, southern North Sea (Germany): Intertidal-supratidal transitions. Between 70 and 20 % of all high tides on yearly average reach or cross mat habitats. Sediments: fine to medium siliciclastic sand. Mats benefit from low-rate sedimentation, but become occasionally buried by landward-directed sedimentation of storm sands (see Figure 2-1-2 (C)). General salinity in the study area 30 - 32 psu. (Figures 2-1-1 (A)-(D); 2-1-2 (A)-(C); 2-1-7 (B)-(F); 2-1-8 (C)-(E); 2-2-1 (H); 2-2-2 (D); 2-3-1 (A); 2-3-3 (A)-(B); 2-3-4 (A)-(B); 2-4-2 (A)-(D))
Selected references: Aigner (1985); Reineck and Gerdes (1997)
Hypersaline sea-marginal ecosystems, Gulf of Aqaba coast (Egypt): o Water-covered lagoon; salinity 100-200 psu; Strong seasonal evaporation causes water level changes which have an effect on light intensity, salinity and temperature within shallow hypersaline water overlying mat surfaces (Figures 2-1-2 (D), (G); 2-2-1 (D), (L); 2-4-1 (A), (E)) o Saline mud flats inundated by trickling water films; salinity 60-100 psu (Figure 2-1-3 (C)) o Higher-lying sabkha plains (Figure 2-4-4 (G))
Selected references: Friedman and Krumbein (1985); Gerdes and Krumbein (1987)
Southern Tunisia coastal bays and sabkhas: Lower supratidal shallows and impondments of 5-25 cm depth filled with concentrated seawater (salinity 60-200 psu); mineral sediments consist of clay and silt mixed with fine to medium-grained quartz sands, oolitic bioclastic sand and evaporites (mainly gypsum) (Figures 2-1-2 (H); 2-1-3 (B); 2-1-4 (A), (D); 2-1-5 (E)-(F); 2-1-6 (B); 2-1-7 (A); 2-1-8 (F); 2-2-1 (J); 2-2-2 (C); 2-3-3 (C), (E); 2-4-2 (E); 2-4-3 (A)-(C))
Selected reference: Noffke et al. (2001)
Saltworks at Bretagne coast (France), on Lanzarote, Canary Islands (Spain) and Formentera, Balearic Islands (Spain): Ponds for evaporation of seawater, in which precipitation of evaporites is less remarkable. Light intensity, temperature and salinity fluctuating in seasonal rhythm with water depth; salinity 60-120 psu. Mineral sediments: clay and silt providing the base for the mats (Figures 2-1-2 (E)-(F); 2-1-4 (C); (F); 2-1-6 (A); 2-2-1 (K); 2-3-1 (C); 2-4-1 (B)-(F))
Selected references: Gerdes et al. (1993); Reineck et al. (1990); Schneider (1995); Schneider and Herrmann (1980)
Lab-cultured system simulating shallow hypersaline lagoonary conditions: Mats inundated by some cm deep hypersaline water; light intensity, temperature and salinity fluctuating with evaporation-related changes of water depths; salinity 60 - 120 psu; mineral base of mats: clay-silt mixture (Figures 2-1-3 (A), (D)-(F), (E); 2-1-4 (B), (E); 2-1-5 (A)-(D); 2-2-1 (A)-(C), (I))
Selected reference: Gerdes and Klenke (2003)

Table 2-1 continued:

Tidal flats and beaches, NE Brazil:
Icapui intertidal flats, fine- to medium-grained siliciclastic sediments and bioclasts Icapui mangals Jericoacoara intertidal beach, medium-grained siliciclastic sediments (Figures 2-1-8 (A)-(B); 2-2-1 (E); 2-3-4 (C)-(D))
Selected reference: Maia (1998)

Figures: Chapter 2

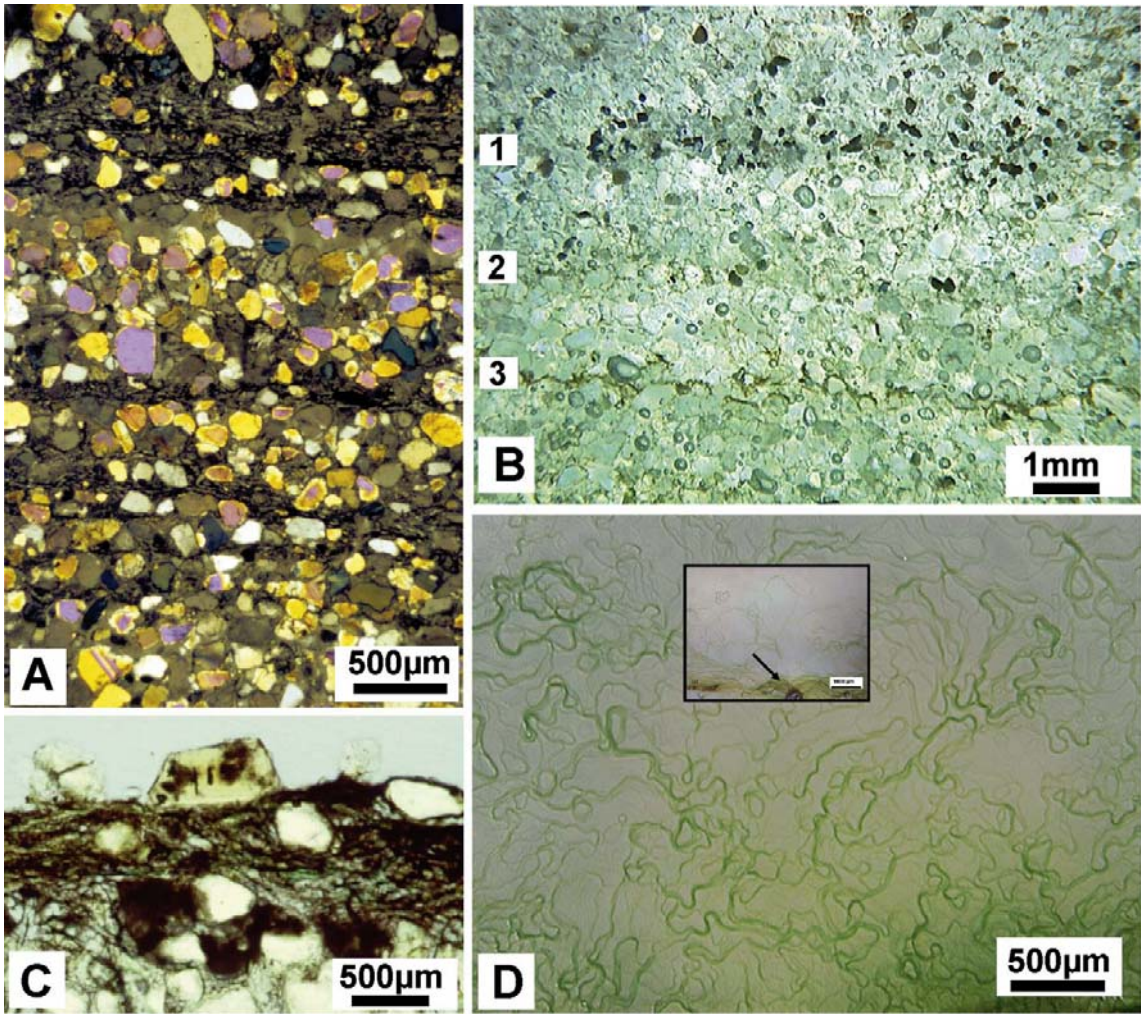

Figure 2-1-1. Biolaminites (single layer view):

(A) Single filamentous mats embedded in quartz-sandy tidal flat deposits. Photo: T. Klenke.

(B) Faint indications of microbial films in quartz-sandy sediment mimicked by lamina-specific heavy mineral grains (lamina no. 1) and iron oxides (laminae no's. 2 and 3). Photo: Gisela Gerdes; modified after photo published in Gerdes et al. (1993).

(C) Vertical section through living microbial network (biodyction) made of filamentous cyanobacteria penetrating pore spaces of siliciclastic sediments. Photo: Photo: Gisela Gerdes; modified after photo published in Gerdes et al. (2000a).

(D) Filaments of *Phormidium* sp., a common mat-forming cyanobacterium, spreading on an agar plate. Small inserted photo: inoculum from where spreading started (arrow). Large photo: 10 days-old stage, filaments amalgamated into bundles and tangles. Succession to coherent mat would need additional time. Photo: modified after one taken by K. Bröhldick.

Locality of photos: (A) to (C) Mellum Island, southern North Sea coast (Germany); (D) experimental set-up.

Figure 2-1-2. Growth bedding:

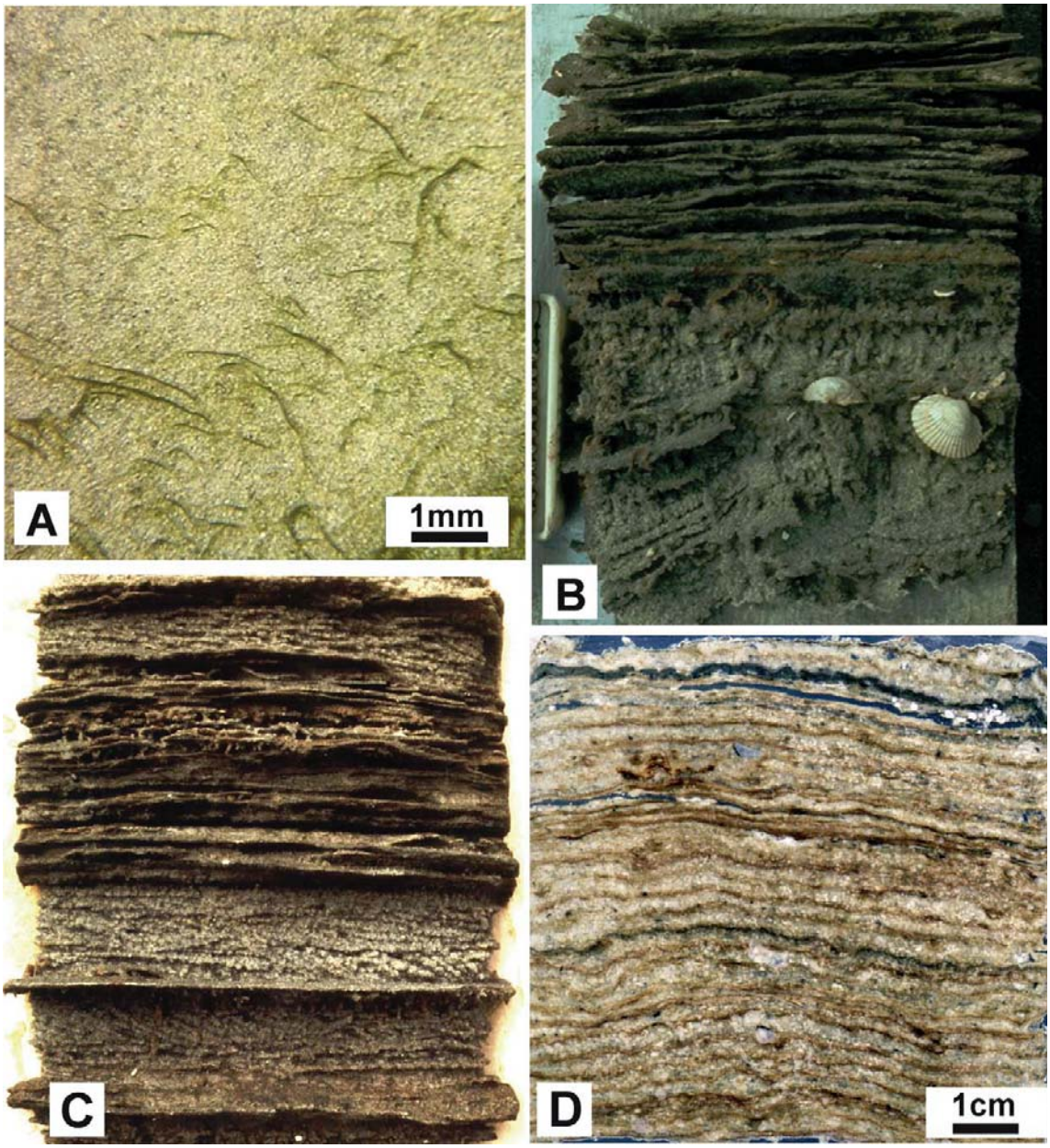

In: *Atlas of microbial mat features preserved within the clastic rock record*, Schieber, J., Bose, P.K., Eriksson, P.G., Banerjee, S., Sarkar, S., Altermann, W., and Catuneau, O., (Eds.), Elsevier, p. 5-38. (2007)

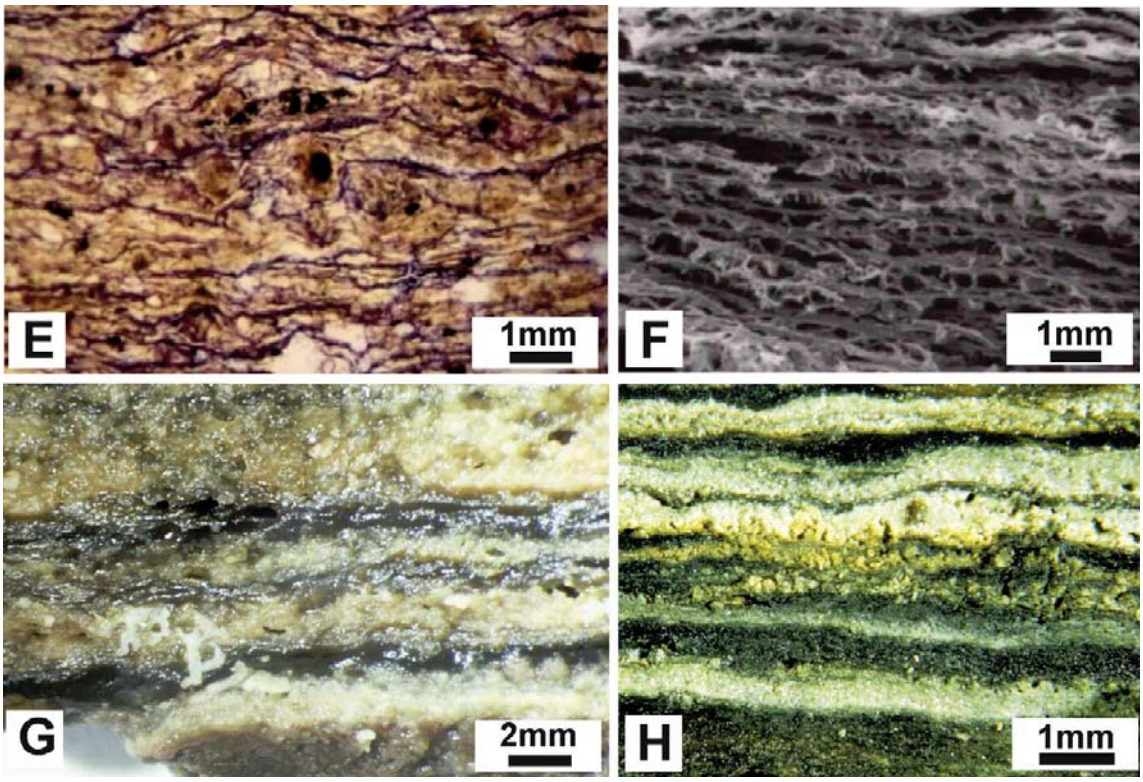

Figure 2-1-2. Growth bedding:

(A) Recolonization of a quartz-sandy surface layer from a preexisting mat underneath, by filaments of the pioneer species *Microcoleus chthonoplastes.* Photo modified after one taken by K. Bröhldick.

(B) Experimental over-sedimentation revealed a stack of twelve mat generations (sharply projecting laminae) that originated from a basic mat cored on top of tidal flat deposits (lower part). Experiment showing the importance of intermittent low-rate sedimentation (relief cast 20 cm high). Photo: Gisela Gerdes; modified after photo published in Gerdes and Krumbein (1987).

(C) Relief cast showing stacks of microbial mats in the middle part, similar to (B), underlain and overlain by cross-stratified sediments (relief cast 30 cm high). Photo: Gisela Gerdes; modified after photo published in Gerdes and Krumbein (1987).

(D) Direct scan of thin section showing shallow water growth-bedding, developed from seasonal over-riding between filamentous cyanobacteria (dark laminae, winter generations) and coccoids (light laminae, summer generations). Type of growth-bedding without the aid of sedimentation (biovarvites). Photo: R. Kiepe.

(E) Thin section of biovarvites showing sequence of filamentous (blue stained) and coccoid mats (yellow interlayers) growing independently from sedimentation. Photo: Gisela Gerdes; modified after photo published in Gerdes et al. (1991).

(F) SEM view of the same material as in (E): Filamentous mats visible, intercalated water-enriched coccoid mats destroyed by critical point drying. Photo: Gisela Gerdes; modified after photo published in Gerdes et al. (1993).

(G) Vertical section through biovarvites showing white laminae overlying thin filamentous mats (dark). Extension of white laminae indicates arid climate influence: surface populations dominated by coccoids excrete large amounts of slime in which carbonates and gypsum precipitated. Dark laminae: winter mats. Photo: Gisela Gerdes.

(H) Vertical section showing biovarvites mixed with subtidal ooid sands (centre) from a nearby lagoon. Yellow colour of grains may indicate weathering products of pyrite. Photo: Nora Noffke.

Locality of photos: (A) to (B) Laboratory-cultured microbial mat; (C) Mellum Island, southern North Sea coast (Germany); (D) Solar Lake, Gulf of Aqaba (Egypt), hypersaline sea-marginal ecosystem; (E) to (F) saltworks, Lanzarote, Canary Islands (Spain); (G) Gavish Sabkha, Gulf of Aqaba (Egypt); (H) Bahar Alouane, southern Tunisia.

In: *Atlas of microbial mat features preserved within the clastic rock record*, Schieber, J., Bose, P.K., Eriksson, P.G., Banerjee, S., Sarkar, S., Altermann, W., and Catuneau, O., (Eds.), Elsevier, p. 5-38. (2007)

Figure 2-1-3. Jelly forms, nodules, biscuits:

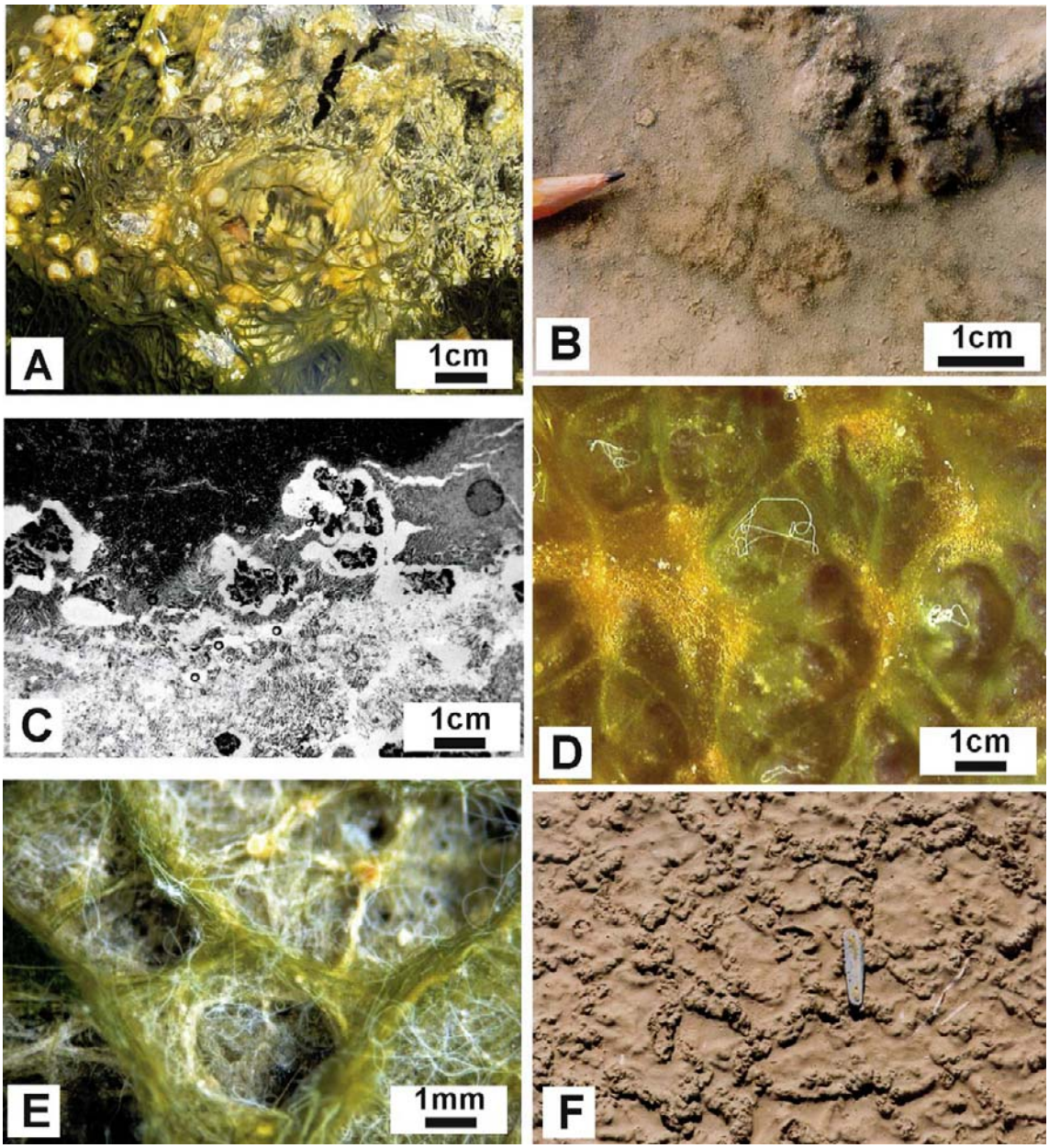

In: *Atlas of microbial mat features preserved within the clastic rock record*, Schieber, J., Bose, P.K., Eriksson, P.G., Banerjee, S., Sarkar, S., Altermann, W., and Catuneau, O., (Eds.), Elsevier, p. 5-38. (2007)

Figure 2-1-3. Jelly forms, nodules, biscuits:

(A) Surface view of a laboratory cultured mat illustrating the over-riding phenomenon; yellow ground: populations of coccoids coloured by photoprotective pigments enriched in EPS; dark green network: filamentous cyanobacteria competing with the coccoids for the most optimal light position. Photo: K. Bröhldick.

(B) Nodular to biscuit-like surface structures produced by local dominance of coccoids. Photo: Nora Noffke.

(C) Internal view of nodular structures made by dominance of coccoids (*Pleurocapsa* sp.), embedded in a fabric of carbonate-coated filamentous sheaths. Photo: Gisela Gerdes; modified after photo published in Gerdes and Krumbein (1987).

(D) Surface view of jelly cushion-like bulges produced by dominance of coccoids, yellow-pigmented slime running into the valleys. Photo: K. Bröhldick.

(E) Nodular surface structures of a shallow water mat surrounded by a network of filamentous cyanobacteria (*Lyngby*a sp.). White filaments: *Beggiatoa*-type chemolithoautotrophic bacteria marking a shift of the O_2-/H_2S chemocline from the inner mat to the mat surface. Photo: Gisela Gerdes.

(F) Salt-encrusted cauliflower-like nodules made by dominance of coccoids projecting over polygonal ridges, about 0.5 to 2 cm high. Knife is 8 cm long. Photo: Nora Noffke; modified after photo published in Noffke et al. (2001).

Locality of photos: (A), (D) to (E) Laboratory-cultured microbial mat; (B) Bou Jemel, southern Tunisia; (C) Gavish Sabkha, Gulf of Aqaba coast (Egypt), hypersaline sea-marginal ecosystem; (F) Bahar Alouane, southern Tunisia.

Figure 2-1-4. Pinnacles, tufts, microstromatolites:

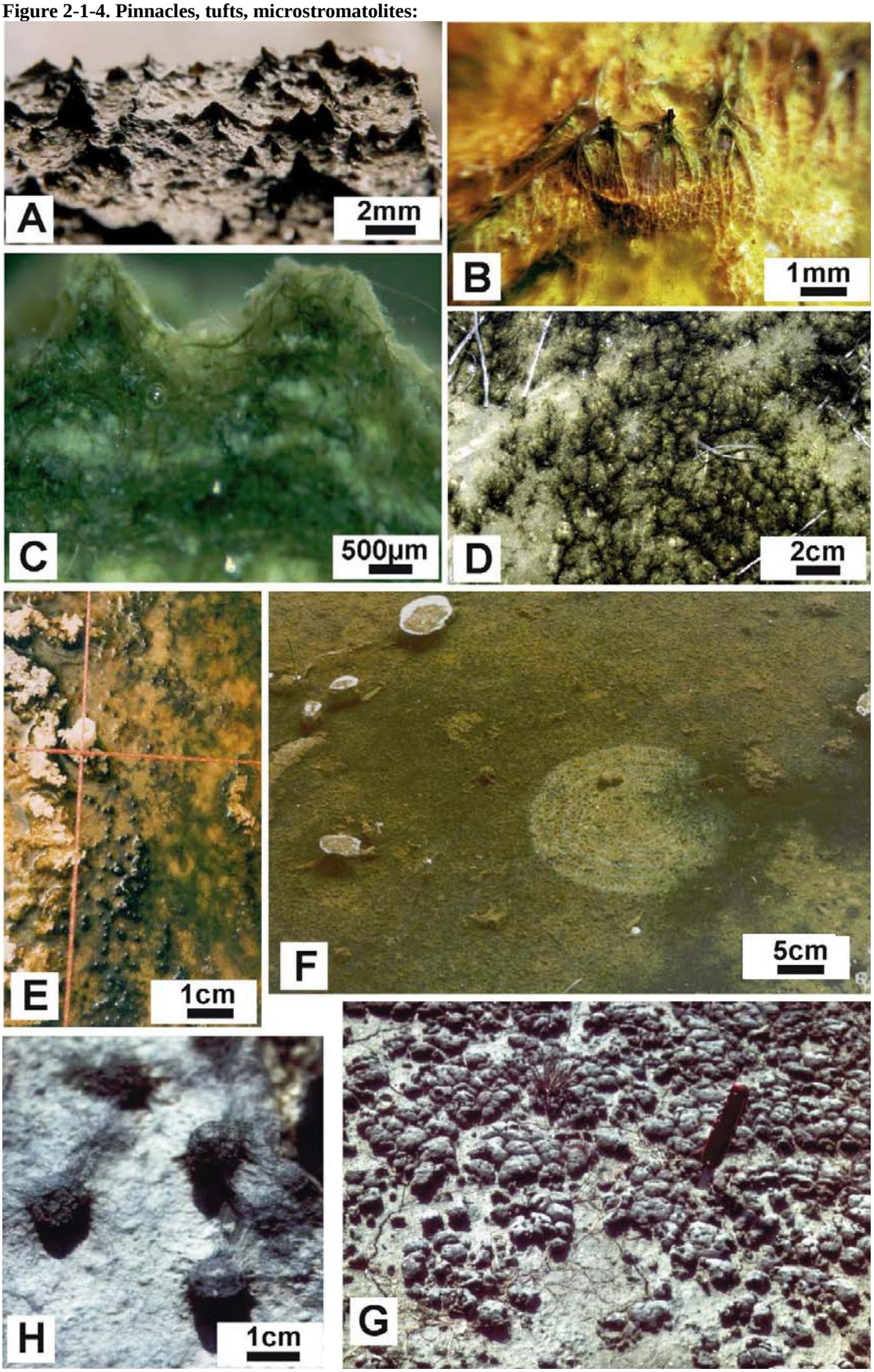

In: *Atlas of microbial mat features preserved within the clastic rock record*, Schieber, J., Bose, P.K., Eriksson, P.G., Banerjee, S., Sarkar, S., Altermann, W., and Catuneau, O., (Eds.), Elsevier, p. 5-38. (2007)

Figure 2-1-4. Pinnacles, tufts, microstromatolites:

(A) Oblique view showing filament tufts of *M. chthonoplastes* standing about 1 mm above the basic mat. Photo: Nora Noffke.

(B) Pinnacles projecting through the mat surface. Basic mat coloured by yellow pigmented slimes. Pinnacles made by dominance of filamentous cyanobacteria (*Lyngbya* sp., *M. chthonoplastes*). Photo: K. Bröhldick (colour-adapted).

(C) Vertical section through basic mat and pinnacles, both made by dominance of *M. chthonoplastes.* Photo: Gisela Gerdes; modified after photo published in Gerdes and Klenke (2003; courtesy of Assoc. Geoaustria).

(D) Local tuft cluster of *M. chthonoplastes* projecting through a flocculous surface mat. Photo: Nora Noffke.

(E) Irregular distribution of pinnacles. Basic mat enriched in yellow pigmented slimes. The photo visualizes polarity change of *M. chthonoplastes* from prostrate-growing filaments (below right) to vertically-erected pinnacles (below left). Laboratory-cultured microbial mat. Photo: K. Bröhldick.

(F) Ring-shaped structures on the surface of a shallow water mat, ring crests crowned by pinnacles. Photo: W.-E. Krumbein.

(G) Knotty surface made by dominance of filamentous cyanobacteria (*Lyngbya aestuarii* ?) which protrude out of the sediment. Knife for scale: 8 cm. Photo by courtesy of J. Schneider.

(H) Individual knots protruding up to 20 mm out of the leathery surface mat. Major species in both the stratiform surface mat and the blister-like knots is the rigid sheath-forming filamentous cyanobacterium *L. aestuarii*. Photo by courtesy of J. Schneider.

Locality of photos: (A), (D) Bahar Alouane, southern Tunisia; .(B), (E) Laboratory-cultured microbial mat; .(C), (F) saltworks, Bretagne coast (France); (G) to (H) saltworks of Secovlje (Gulf of Piran, Slovenia).

Figure 2-1-5. Reticulate surface patterns:

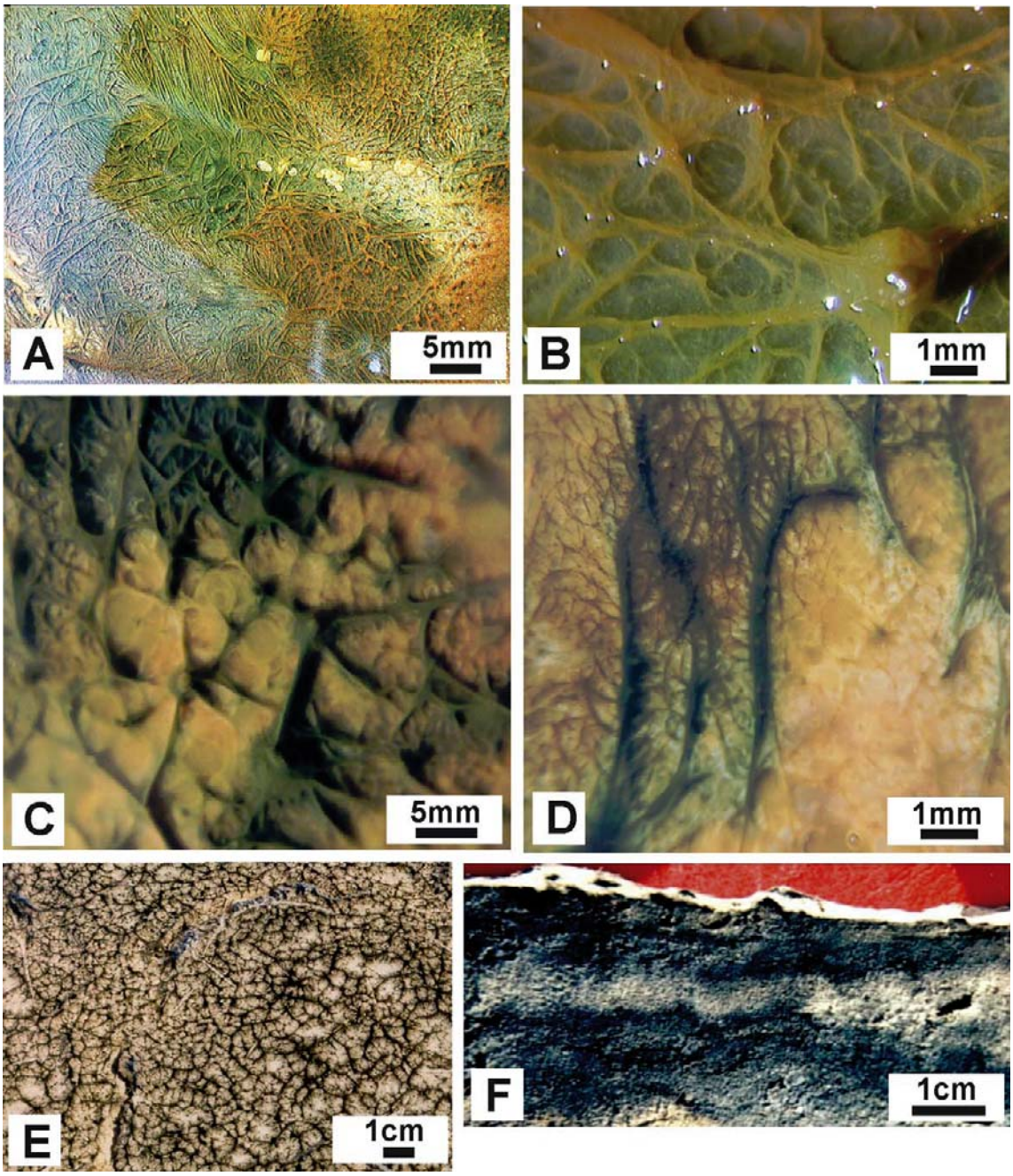

In: *Atlas of microbial mat features preserved within the clastic rock record*, Schieber, J., Bose, P.K., Eriksson, P.G., Banerjee, S., Sarkar, S., Altermann, W., and Catuneau, O., (Eds.), Elsevier, p. 5-38. (2007)

Figure 2-1-5. Reticulate surface patterns:

(A) Reticulated patterns made of intersecting bulges and pinnacles established on a microbial mat surface. Photo: K. Bröhldick (colour-adapted); modified after photo published in Gerdes and Klenke (2003; courtesy of Assoc. Geoaustria).

(B) Close-up of (A): Pinnacles form the focus of radial bulges. Photo: K. Bröhldick; modified after photo published in Gerdes and Klenke (2003; courtesy of Assoc. Geoaustria).

(C) Small-scale reticulated mat surface produced by lateral dominance changes between coccoids (jelly cushion-like features) and filaments (tufts, pinnacles, bulges). Photo: K. Bröhldick.

(D) Thick bulges made by the filamentous cyanobacterium *Lyngbya* sp. and smaller reticulated veins stretching over a yellow layer of slime-embedded coccoids. Photo: K. Bröhldick.

(E) Macroscopic surface view of a reticulated microbial mat resembling “elephant skin”. Photo: Nora Noffke; modified after photo published in Gerdes et al. (2000b).

(F) Vertical section revealing counterparts of reticulated surface mat (top) and wavy-crinkly bounding planes in the sediment below. Photo: Nora Noffke.

Locality of photos: (A) to (D) Laboratory-cultured microbial mat; (E) to (F) Bahar Alouane, southern Tunisia.

Figure 2-1-6. Polygonal bulges, convoluted structures:

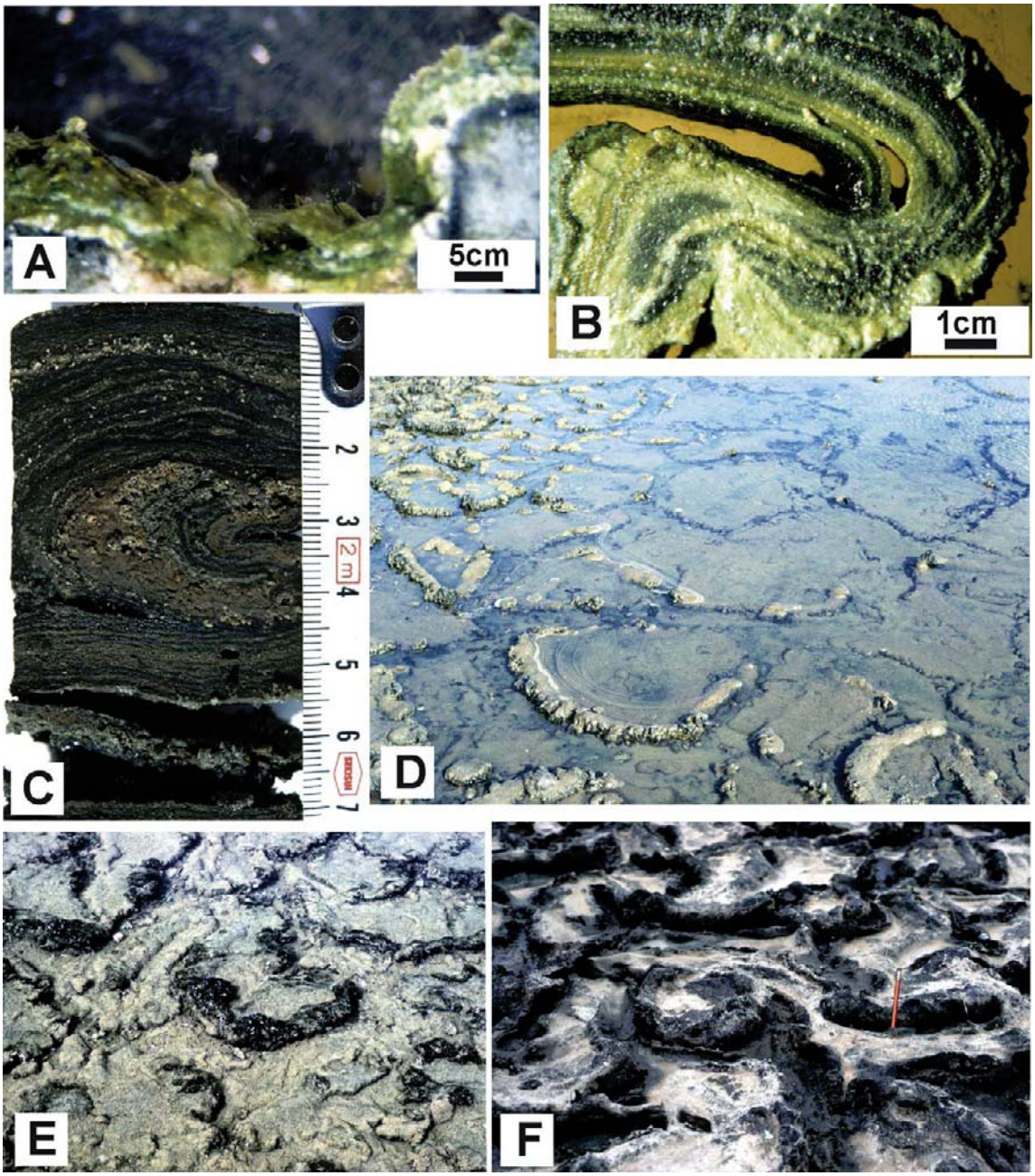

In: *Atlas of microbial mat features preserved within the clastic rock record*, Schieber, J., Bose, P.K., Eriksson, P.G., Banerjee, S., Sarkar, S., Altermann, W., and Catuneau, O., (Eds.), Elsevier, p. 5-38. (2007)

Figure 2-1-6. Polygonal bulges, convoluted structures:

(A) Microbial mat growing into a shrinkage crack. Pinnacles on the base of the crack (left). Dominant genera: *Microcoleus, Oscillatoria*. Photo: Gisela Gerdes.

(B) Vertical section through a pocket-like multilayered crack tapestry produced by microbial mats that grew from the surrounding mat into a shrinkage crack. Photo: Nora Noffke; modified after photo published in Gerdes et al. (2000a).

(C) Sectional view of sediment core showing involute growth bedding. Photo: K. Dunajtschik-Piewak; modified after photo published in Gerdes et al. (1994a).

(D) Water-covered microbial bulges marking polygonal cracks. Photo: K. Dunajtschik-Piewak.

(E) Irregular surface patterns due to the bulging growth of mats as a reaction to cracking and subsequent flooding. Some individual mat fragments partly over-flipped. Photo: K. Dunajtschik-Piewak.

(F) Extraordinary thick polygonal bulges within abandoned salina basin. Prolonged periods of overstanding calm and warm seawater alternating with shorter periods of drying may have produced these growth structures (pencil 17 cm long). Photo: K. Dunajtschik-Piewak.

Locality of photos: (A) saltworks, Bretagne coast (France); (B) Bahar Alouane, southern Tunisia; (C) to (F) saltworks Lanzarote, Canary Islands (Spain).

Figure 2-1-7. Microbial binding structures:

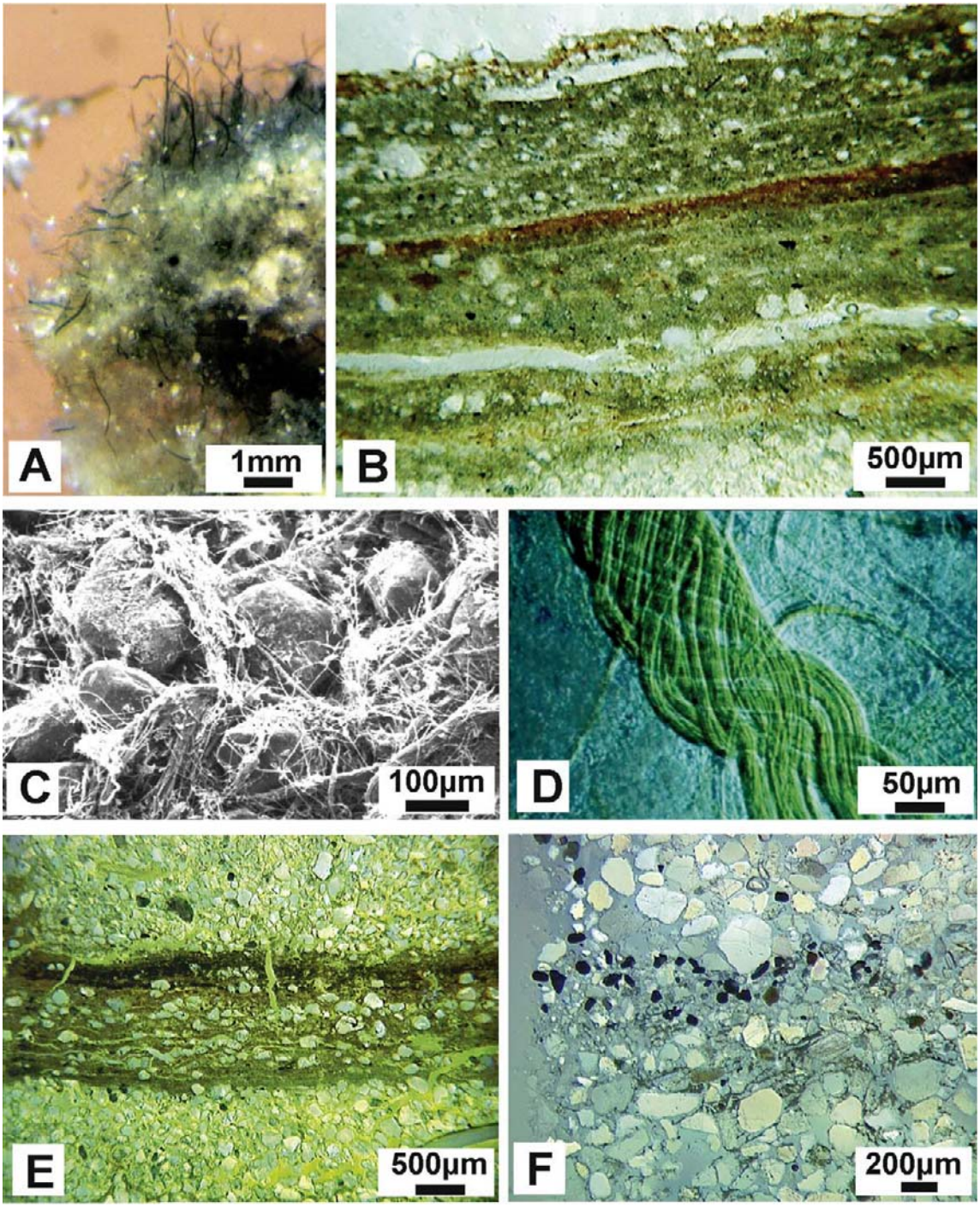

In: *Atlas of microbial mat features preserved within the clastic rock record*, Schieber, J., Bose, P.K., Eriksson, P.G., Banerjee, S., Sarkar, S., Altermann, W., and Catuneau, O., (Eds.), Elsevier, p. 5-38. (2007)

Figure 2-1-7. Microbial binding structures:

(A) White amorphous carbonate cluster enriched in microbial fabrics due to baffling effects of upright colonies of filamentous cyanobacteria. Photo: Nora Noffke.

(B) Vertical section of a thick multilayered surface mat overlying a quartz-sandy layer. A few sand grains are bound internally and on top of the mat surface. Photo: Gisela Gerdes.

(C) SEM view of quartz grains bound by filamentous microbial surface mat. Photo: Gisela Gerdes.

(D) Light microscopy showing an elongated, twisted sheath bundle of *M. chthonoplastes*, a species particularly capable of sediment binding. Photo: Gisela Gerdes; modified after photo published in Gerdes and Klenke (2003; courtesy of Assoc. Geoaustria).

(E) Biolaminite within quartz sandy tidal flat sediments, containing matrix-supported sediment grains arranged with their long axes parallel to the bounding plane. Photo: Gisela Gerdes.

(F) Microbial lamina-bound heavy mineral grains within siliciclastic tidal flat sediments. Photo: Gisela Gerdes.

Locality of photos: (A) Bahar Alouane, southern Tunisia; (B) to (F): Mellum Island, southern North Sea coast (Germany).

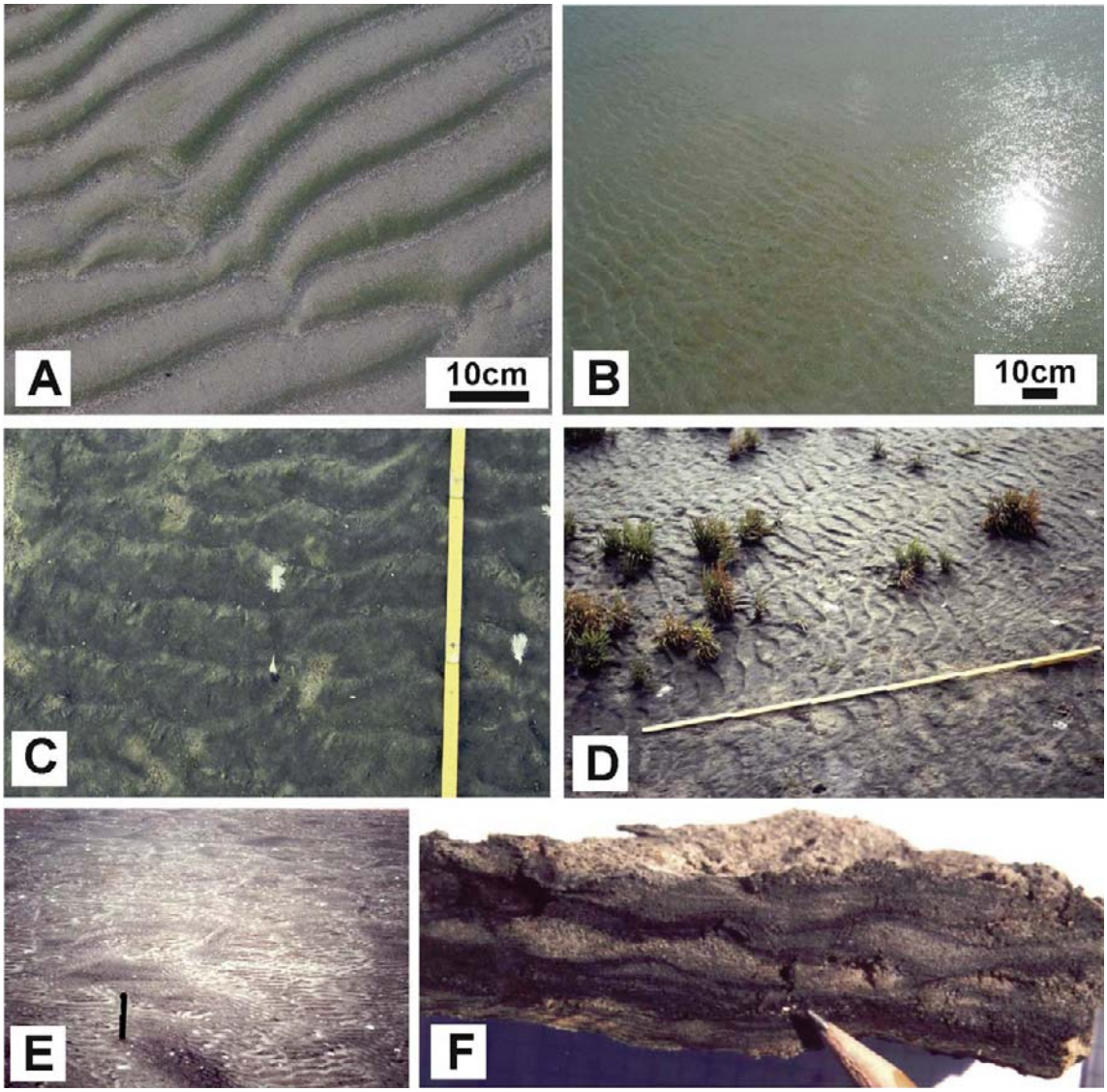

Figure 2-1-8. Overgrowth, fixation and nivellement of ripples:

(A) Surface of intertidal beach sand. Thin microbial biofilms cover the flanks of asymmetric oscillation ripples. Photo: B. Petzelberger.

(B) Surface of an intertidal sand flat. Small asymmetric current ripples covered by a slightly increasing microbial biofilm. Photo: B. Petzelberger.

(C) Advanced microbial growth overprinting asymmetric ripples. Photo: Nora Noffke.

(D) Rippled surface of high-lying tidal flats completely overprinted and stabilized by a highly productive microbial mat. Photo: Nora Noffke; modified after photo published in Noffke (1997).

(E) Multidirectional ripple marks generated from changes between physical sedimentation and microbial colonization and fixation of ripple marks. Photo: Nora Noffke; modified after photo published in Gerdes et al. (2000a) and Noffke (1998).

(F) Cross-section through surface sediments showing structures resembling lenticular bedding. Mats of different thickness have overgrown ripple crests, flanks and valleys indicating that the microtopography of ripples is of ecologic importance (tip of pencil 1 cm long). Photo: Nora Noffke.

Locality of photos: (A) to (B) Icapui tidal flats, NE Brazil; (C) to (E) Mellum Island, southern North Sea coast (Germany); (F) Zarzis beach, southern Tunisia.

Figure 2-2-1. Mat-confined gas bubbles:

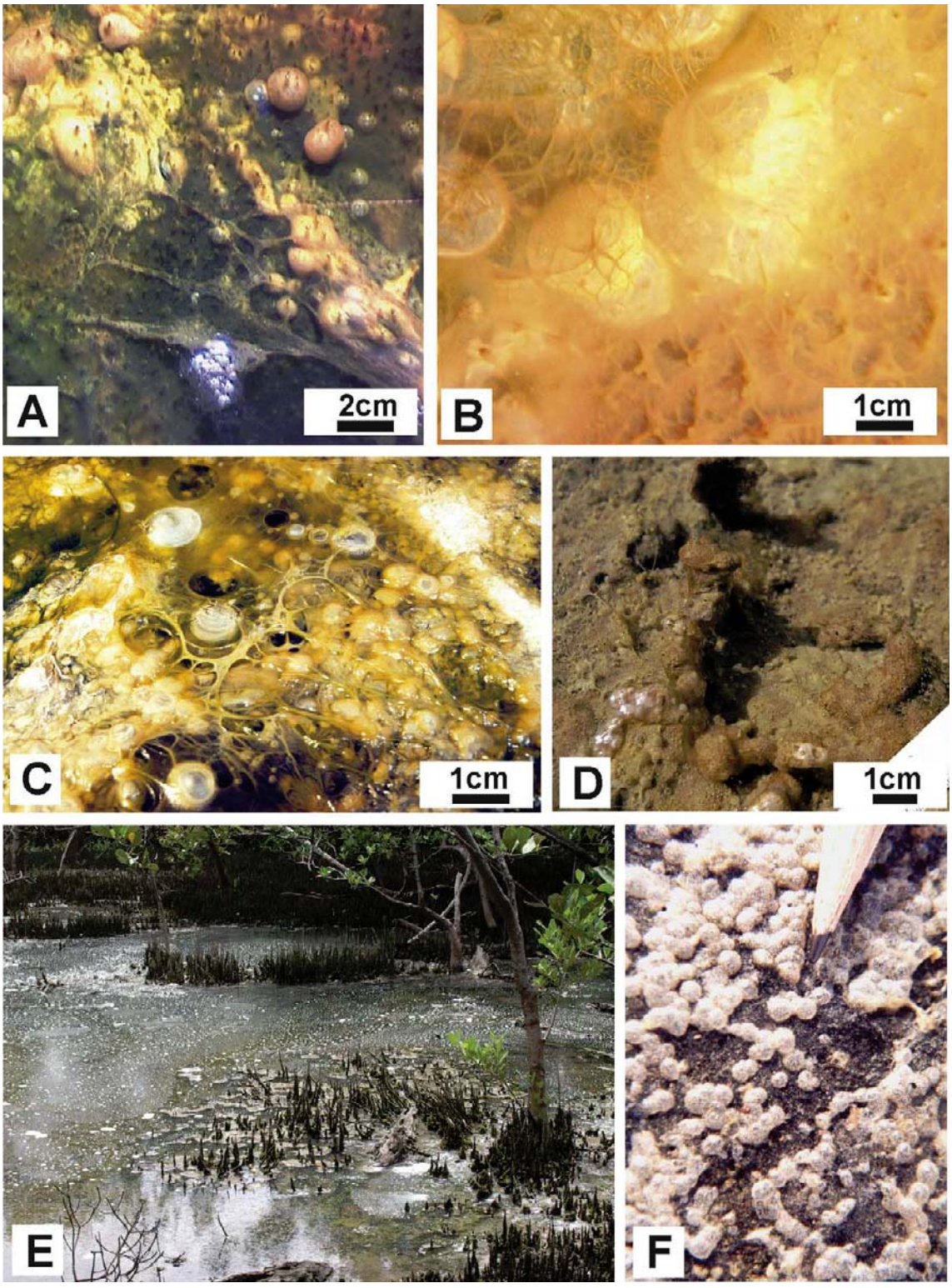

In: *Atlas of microbial mat features preserved within the clastic rock record*, Schieber, J., Bose, P.K., Eriksson, P.G., Banerjee, S., Sarkar, S., Altermann, W., and Catuneau, O., (Eds.), Elsevier, p. 5-38. (2007)

Figure 2-2-1. Mat-confined gas bubbles:

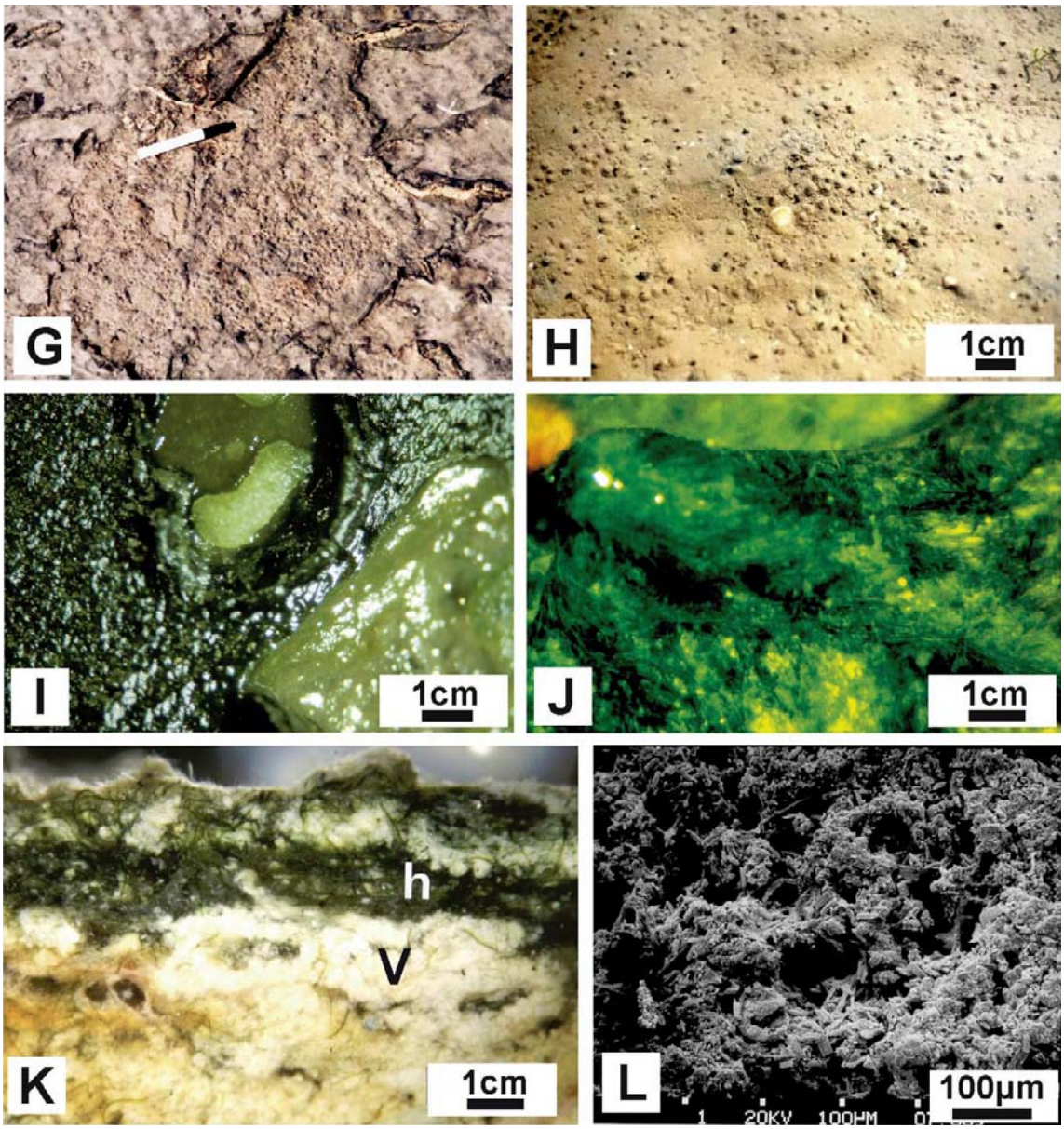

In: *Atlas of microbial mat features preserved within the clastic rock record*, Schieber, J., Bose, P.K., Eriksson, P.G., Banerjee, S., Sarkar, S., Altermann, W., and Catuneau, O., (Eds.), Elsevier, p. 5-38. (2007)

Figure 2-2-1. Mat-confined gas bubbles:

(A) Surface of a shallow water mat built-over by slime threads and bubbles. Bubbles coated by biofilms. Pinnacles grow on bubble surfaces and the basic mat. Photo: K. Bröhldick (colour-adapted).

(B) Close-up of bubbles captured by biofilm. In the thin radial ridges and small pinnacles growing on bubble surfaces, small filamentous species (*Spirulina* sp.) are abundant. Photo: E. Ahrensfeld (colour-adapted); modified after photo published in Gerdes and Klenke (2003; courtesy of Assoc. Geoaustria).

(C) Three-dimensional scum expanding from the surface of a shallow water mat into the surficial water. Slime-enriched threads, films and bubbles provide various interfaces and 3D spaces for the bacterial front to move into the pelagic realm. Photo: E. Ahrensfeld (colour-adapted); modified after photo published in Gerdes and Klenke (2003; courtesy of Assoc. Geoaustria).

(D) Similar 3D structures building over the surface of hypersaline shallow water mats. In biofilms coating bubbles, diatoms are abundant. Reticulate patterns cover bubble surfaces. Deeper holes (centre) favour growth of green-pigmented filamentous mats. Photo: W.-E. Krumbein.

(E) Benthic microbial mats projecting into the water column of a mangal pool using their own metabolic products (bubbles, scums, slimes, flocs) as interfaces for colonization. Photo: B. Petzelberger.

(F) Froth on a dark mat surface left behind after complete evaporation of shallow water stands. Bubbles are “frozen” by biofilm-coatings. Pencil tip 1 cm long. Photo: Nora Noffke.

(G) Surface of a widely cracked desiccating mat. Blistered crack-bottom indicating subsurface metabolic effects. Mat remains at left and right. Photo: Nora Noffke.

(H) Blisters 0.5 to 1 mm high project above a thin cohesive sand layer. Photo: H.-E. Reineck.

(I) Blister including a dumbbell-shaped gypsum precipitate embedded in polysaccharide slime (bubble punctured to look inside). Blisters formed by gypsum precipitates are described by Golubic (1973). Photo: Gisela Gerdes.

(J) Bubbles turning out filamentous meshworks giving rise to pinnacle formation. Photo: Nora Noffke.

(K) Cross-section through multilaminated mat surface including horizontally oriented filamentous (h) and vertically extended mat horizons (v). Various bubbles dispersed in the white amorphous organic layer. Photo: Gisela Gerdes.

(L) SEM view of internal microbial fabric containing a small hollow sphere (probably a bubble), surface coated by diatoms, and bacteria producing stabilizing slime coating the surface of the sphere. Photo: W.-E. Krumbein; modified after photo published in Gerdes et al. (1994b).

Locality of photos: (A) to (C) Laboratory-cultured microbial mat; (D) Gavish Sabkha, Gulf of Aqaba coast (Egypt), hypersaline sea-marginal ecosystem; (E) Icapui mangals, NE Brazil; (F) Sabkha Bou Jemel, southern Tunisia; (G), (J) Bahar Alouane, southern Tunisia; (H) Mellum Island, southern North Sea coast (Germany); (I) Laboratory-cultured microbial mat; (K) saltworks, Bretagne coast (France); (L) Solar Lake, Gulf of Aqaba coast (Egypt), hypersaline sea-marginal ecosystem.

Figure 2-2-2. Layered iron enrichment:

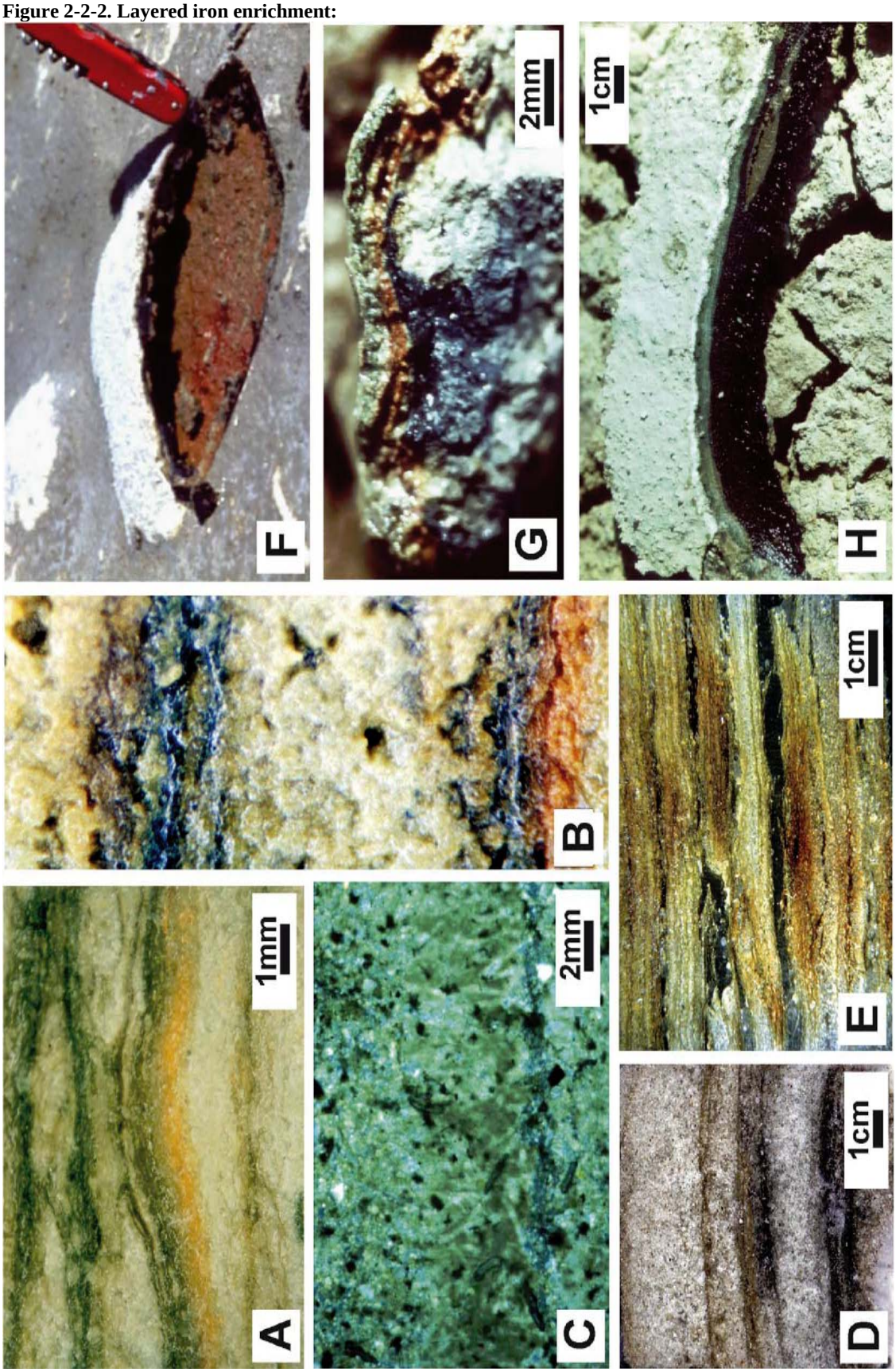

In: *Atlas of microbial mat features preserved within the clastic rock record*, Schieber, J., Bose, P.K., Eriksson, P.G., Banerjee, S., Sarkar, S., Altermann, W., and Catuneau, O., (Eds.), Elsevier, p. 5-38. (2007)

Figure 2-2-2. Layered iron enrichment:

(A) Cross-section through a filament-dominated surface mat (*M. chthonoplastes* dominant). Iron hydroxide horizon developed below the filamentous photosynthetic mat. Photo: Gisela Gerdes.

(B) Deeper core section 5 to 10 cm below aerial surface. Mats enriched in organic matter appear black from ferrous iron (FeS). Lower mat horizon underlain by a ferric iron horizon. Photo: Gisela Gerdes.

(C) Thin section microphotograph showing lamina-bound pyrite below a horizon of vertically to diagonally oriented microbial sheaths. Pyrite is also distributed between the sheaths. Photo: Nora Noffke; modified after photo published in Noffke et al. (2003a).

(D) Direct scan of a thin section of quartz-sandy tidal flat sediments prepared from deeper core material about 15 cm below aerial surface. Strongly reduced mat horizons (below) reveal metabolic activity of sulphate-reducing bacteria, brownish iron horizons of hydrous iron oxides mimick former microbial mats (above). Photo: R. Kiepe.

(E) Cross-section through core material showing heterogeneous nucleation sites for metal oxide deposition within biolaminites mixed with clay minerals, ooid grains, microbial cells, sheaths and capsules. Photo: Nora Noffke.

(F) Vertical section through an aragonite-covered gas dome developed in a surface mat. The opening allows the view onto the subsurface layer which is coloured by rusty-brown iron-oxide-hydrate. According to the model of iron mobilization in microbial mats (Schneider and Herrmann, 1980), Fe^{++} (aqu) is able to migrate upwards from pore water within anoxic mats and anaerobic clay underneath the redox-discontinuity-layer (RDL) and precipitates as Fe^{+++} above RDL. Photo by courtesy of J. Schneider.

(G) Vertical section through wavy microbial mat which covers organics and clay like a carpet (also termed “petola” by the salt workers). Blue-green top mat dominated by *M. chthonoplastes*. Rusty-brown layer between top mat and anoxic sediment underneath indicates Fe^{+++} formation above RDL-layer .Salt workers take care to keep the petola intact (for techniques to avoid Fe^{+++} discolouration of NaCl precipitating from brines see Schneider and Herrmann, 1980) . Photo by courtesy of J. Schneider.

(H) Parts of the surface (top and below) surrounding a fresh crack (middle) in microbial mat. Note the black reduced material made visible by the crack reaching up to the blue-green cyanobacterial top mat. White cover: aragonite, freshly precipitated from surficial seawater. Photo by courtesy of J. Schneider.

Locality of photos: (A) to (B) saltworks, Bretagne coast (France); (C) Bahar Alouane, southern Tunisia; (D) Mellum Island, southern North Sea coast (Germany); (E) lagoon of Bou Grara, southern Tunisia; (F) to (H) saltworks, Secovlje, Gulf of Piran, Slovenia (increasing hypersalinity from (F) to (H).

Figure 2-2-3. Patterns resembling Kinneyia:

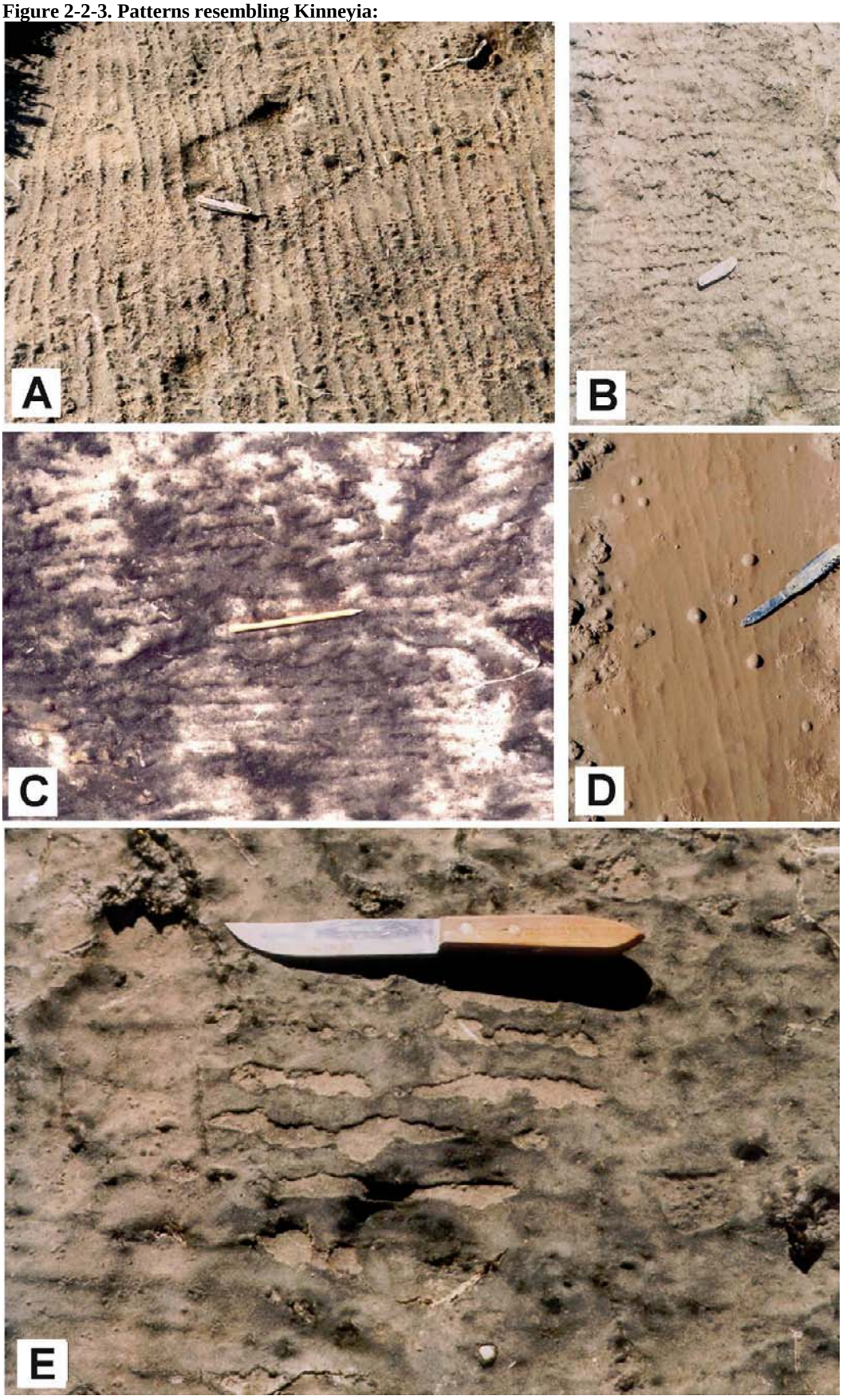

In: *Atlas of microbial mat features preserved within the clastic rock record*, Schieber, J., Bose, P.K., Eriksson, P.G., Banerjee, S., Sarkar, S., Altermann, W., and Catuneau, O., (Eds.), Elsevier, p. 5-38. (2007)

Figure 2-2-3. Patterns resembling Kinneyia:

(A) Plane surface view of small elongated parallel ridges 0.5 to 1 cm wide, forming a regular pattern. Blisters line the crests. Knife is 8 cm long. Photo: Nora Noffke.

(B) Small ridges only a few centimetres in length running only partly parallel to each other, some are curved and merge with adjacent ridges. Trapped blisters again correspond to the crests. Photo: Nora Noffke.

(C) Slightly damp surface conditions favour buried mat organisms to overgrow ripples from below. Photo: Nora Noffke.

(D) From gently elevated margins occupied by coccoids forming characteristic cauliflower-like nodules (example at left), microbial slimes moved into the shallow topographic low (centre). Slow gravity gliding of the sluggish surface composed of bacteria, slime-agglutinated clay and gypsum causes fine elongated folds similar to table cloths. Gas bubbles from metabolic activities of the mat below are captured by the sluggish surface. Photo: Nora Noffke; modified after photo published in Gerdes et al. (2000a).

(E) Cracking taking place along crests of the hollow ridges after drying. Photo: Nora Noffke.

Locality of photos: (A) to (E) Bahar Alouane, southern Tunisia..

Figure 2-3-1. Shrinkage cracks:

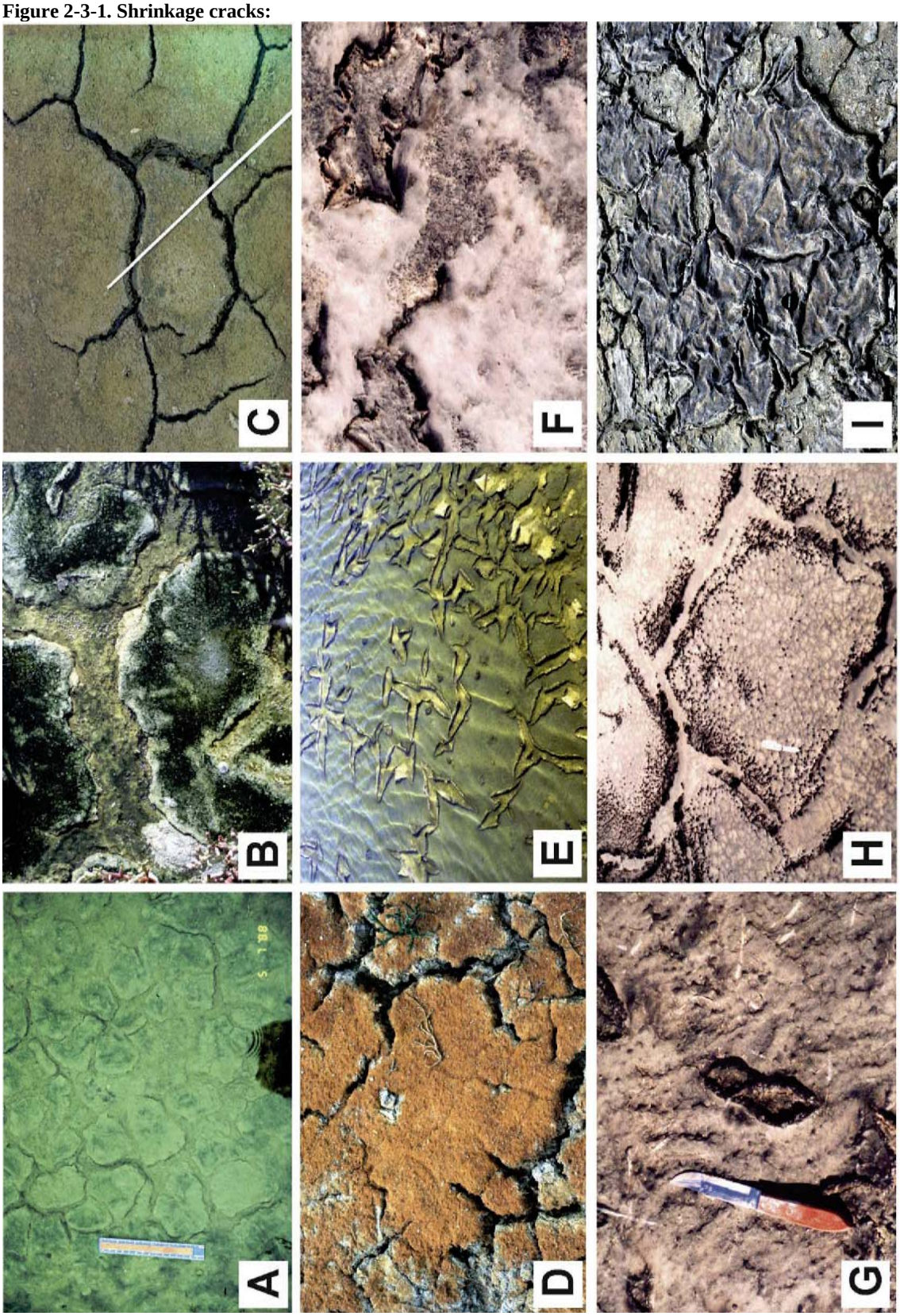

In: *Atlas of microbial mat features preserved within the clastic rock record*, Schieber, J., Bose, P.K., Eriksson, P.G., Banerjee, S., Sarkar, S., Altermann, W., and Catuneau, O., (Eds.), Elsevier, p. 5-38. (2007)

Figure 2-3-1. Shrinkage cracks:

(A) Polygonal cracks in a thin microbial mat growing on quartz-sandy tidal flats. Sand base exposed by widely spaced cracks, clefts re-colonized by microbial films after re-wetting. Photo: H.-E. Reineck.

(B) Polygonal cracks in a thin microbial mat growing on a mixture of clay and gypsum mush. Widely spaced cracks expose the underlying sediment. Oxygen bubbles in the cracks indicate photosynthetic activity of biofilms after flooding. Photo: J. Gifford.

(C) Cracks within a thick microbial mat growing on clay. Compare deep-reaching cracks and narrow clefts with wide shallow cracks in thin mats (B). Photo: J. Gifford.

(D) Partly incomplete cracks within a thick microbial mat, polygon surfaces covered by filaments coated by iron oxides during drying. Filamentous meshwork triggered crack patterns, similar to tearing blotting paper. Photo: J. Gifford.

(E) Subaqueous clay and gypsum sediment covered by a thin mat loosely attached to the substrate. Spindle-like cracks caused by bird traces. Photo: J. Gifford.

(F) Unusual kind of non-orthogonal, incomplete cracks formed in a mixture of terrestrial mud and gypsum glued together by microbial slimes (surface sediments are white smooth areas). Crack resembles a bird's foot; note the curled-up edges. Photo: Nora Noffke.

(G) Crack morphology resembling a bird's foot, developed in pseudo-rippled and blistered surface patterns of a mat (table cloth-like features, see Figure 2-2-3). Knife is 20 cm long. Photo: Nora Noffke.

(H) Widely spaced polygonal cracks, margins elevated due to microbial bulges (see Figure 2-1-6) and contoured by pinnacles (Figure 2-1-4) confined to polygon edges. Reticulate patterns (Figure 2-1-5) shimmer through a mixture of salt crystals and microbial slimes covering polygon surfaces. Knife is 15 cm long. Photo: Nora Noffke; modified after photo published in Gerdes et al. (2000a).

(I) Surface of a desiccated and cracked mat, with shrinkage exposing the clay-mineral substrate marked by orthogonal cracks, while the overlying mat shows unusual crack morphologies, incomplete fissures, folds and upcurled margins. Abandoned salina basin (cap = 5 cm in diameter). Photo: H.-E. Reineck.

Locality of photos: (A) Mellum Island, southern North Sea coast (Germany); (B) to (E) saltworks, Bretagne coast (France); (F) to (G) Bahar Alouane, southern Tunisia; (H) Sabkha Bou Jemel, southern Tunisia; (I) saltworks, Lanzarote, Canary Islands (Spain).

Figure 2-3-2. Jelly-rolls, flip-overs:

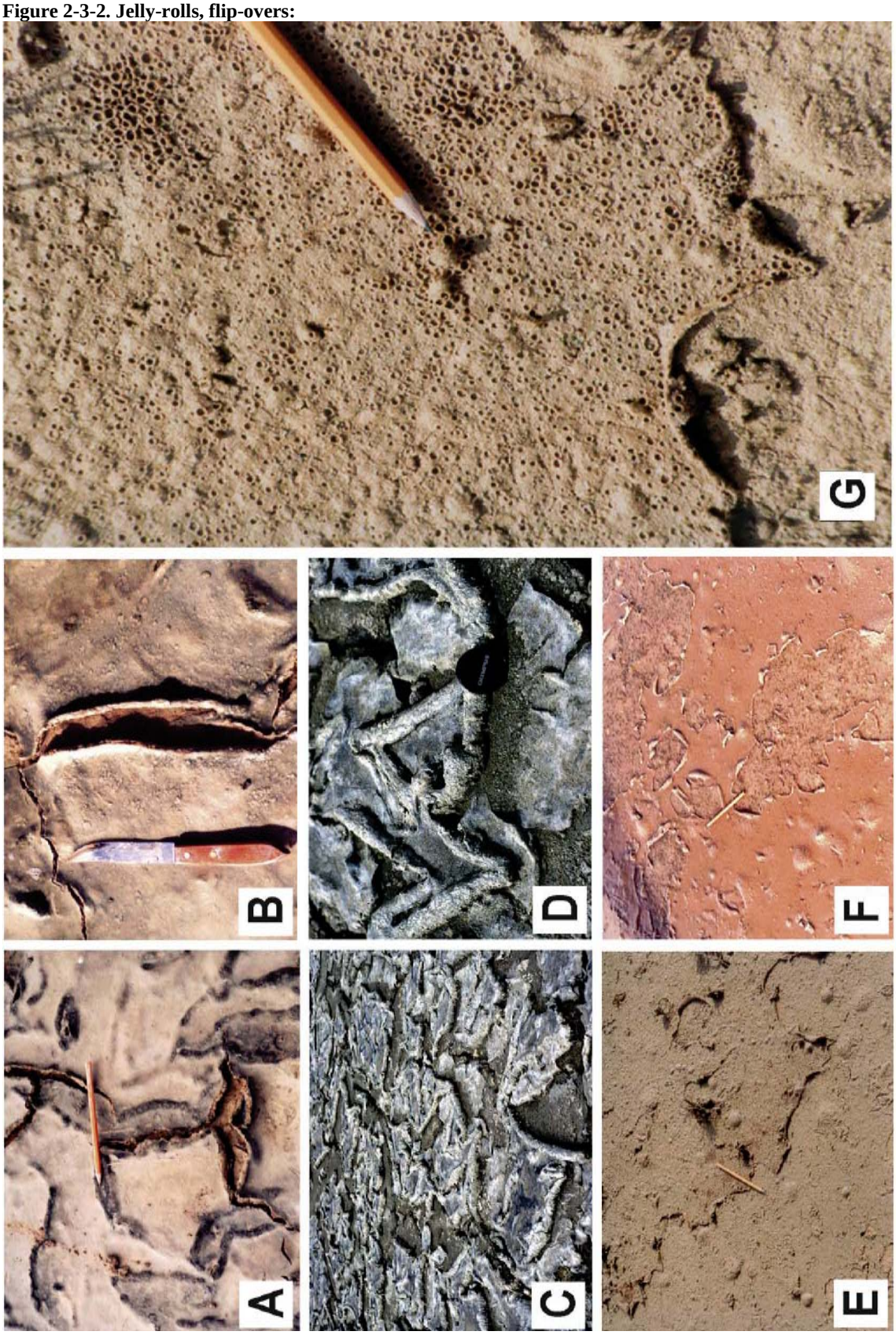

In: *Atlas of microbial mat features preserved within the clastic rock record*, Schieber, J., Bose, P.K., Eriksson, P.G., Banerjee, S., Sarkar, S., Altermann, W., and Catuneau, O., (Eds.), Elsevier, p. 5-38. (2007)

Figure 2-3-2. Jelly-rolls, flip-overs:

(A) Healed-up and new spindle-like cracks in jelly mats dominated by coccoids and enriched in slime-agglutinated gypsum (white areas). Note healed-up cracks guiding new crack directions. Crack margins roll up tightly as they dry. The rusty red colour underneath may be due to the precipitation of iron hydroxides above RDL layer. Pencil = 17 cm in length. Photo: Nora Noffke.

(B) Close-up of elongated spindle-like crack, margins rolled-up (knife is 20 cm long). Photo: Nora Noffke.

(C) Surface patterns of a dessicated and widely cracked microbial mat loosely attached to the substrate, polygon margins rolled-up after drying (cap = 5 cm in diameter). Photo: H.-E. Reineck.

(D) Close-up of (C): crack margins giving rise to mat curls. Photo: H.-E. Reineck; modified after photo published in Gerdes et al. (1993).

(E) Jelly surficial biofilm cracked due to drying; gas bubbles indicate metabolic activity of mat-forming organisms (similar occurrences revealed contents of CO_2 and CH_4. within the bubbles - Schneider, personal communication). Pencil in (E) – (G) = 17 cm in length. Photo: Nora Noffke.

(F) Similar biofilm as in (E). Gas bubbles aerating the jelly mat from below may support mat detachment. Upcurled margins producing jelly-rolls, some on top of the mat. Photo: Nora Noffke.

(G) Edges of loosely attached biofilm partly overflipped and rolled up. Flip-over exposing mat underside, the jelly material being occupied by various burst-open bubbles supporting detachment processes. Photo: Nora Noffke.

Locality of photos: (A), (F) Sabkha Amchoun, southern Tunisia; (B) Sabkha Bou Jemel, southern Tunisia; (C) to (D) saltworks of Lanzarote, Canary Islands (Spain); (E), (G) Sidi Slim, Djerba, southern Tunisia.

Figure 2-3-3. Erosional edges, mat chips:

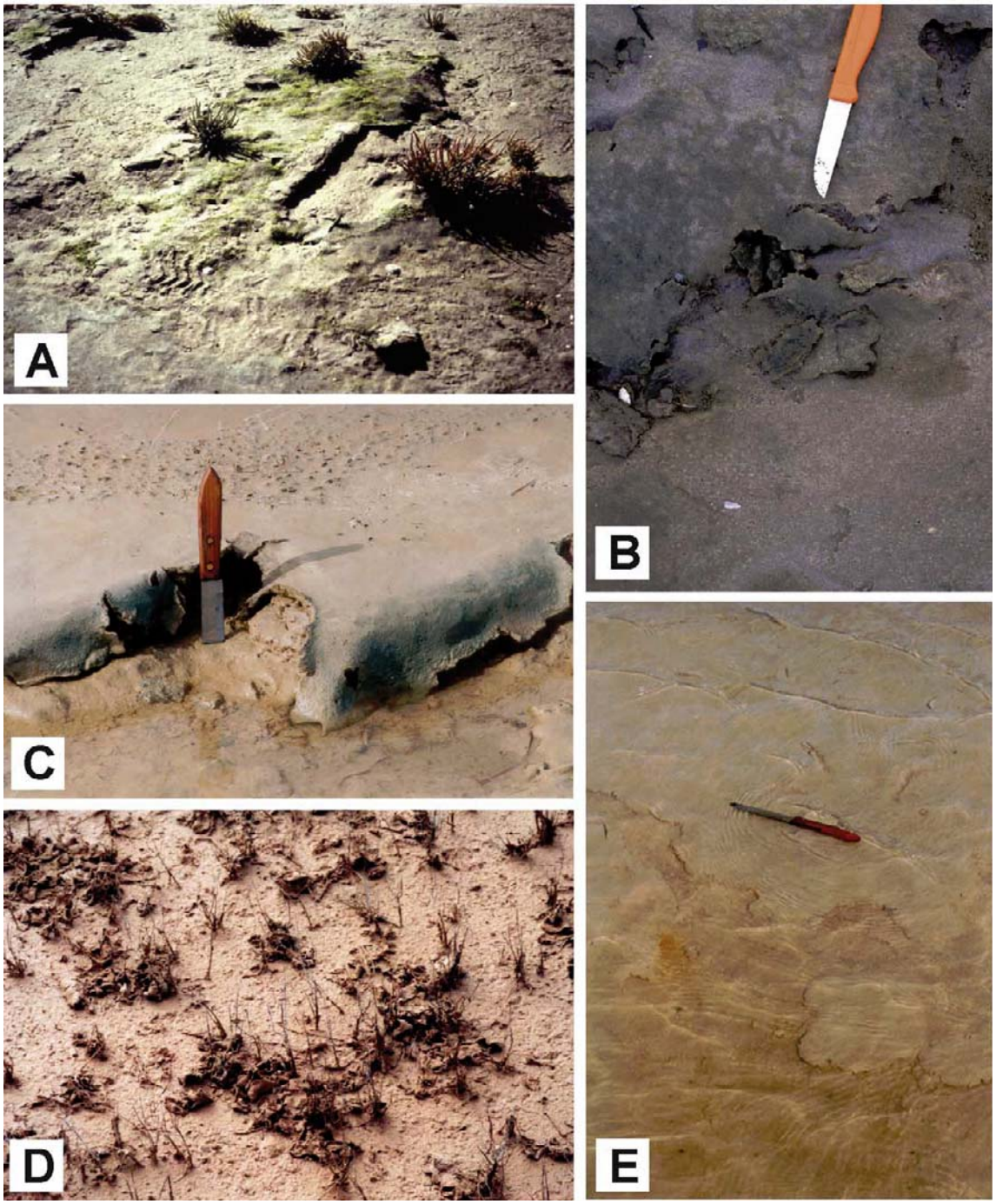

In: *Atlas of microbial mat features preserved within the clastic rock record*, Schieber, J., Bose, P.K., Eriksson, P.G., Banerjee, S., Sarkar, S., Altermann, W., and Catuneau, O., (Eds.), Elsevier, p. 5-38. (2007)

Figure 2-3-3. Erosional edges, mat chips:

(A) Microbial mat hanging over the edge of an erosional depression (right) giving rise to the genesis of mat chips (biostabilized quartz-sandy tidal flats). Photo: Nora Noffke.

(B) Microbial sand chips drop off the undermined mat (knife is 20 cm long). Photo: Nora Noffke.

(C) Coherent mat made of coccoidal and filamentous cyanobacteria hangs over a small terraced cliff undermined by water agitation. Structure marking the shoreline of a hypersaline lagoon. Some mat chips lie upside down on muddy substrate of the lower terrace. Photo: Nora Noffke.

(D) Microbial mat chips accumulating behind stands of halophytes. Photo: Nora Noffke.

(E) Subaqueous erosion-edge of mat, and reworking of mat; loose and thin mats growing on soft muddy sediments producing fragile mat chips. Photo: Nora Noffke.

Locality of photos: (A) to (B) Mellum Island, southern North Sea coast (Germany); (C) Sabkha Bou Jemel, southern Tunisia; (D) Sidi Slim, Djerba, southern Tunisia; (E) Sabkha Bou Jemel, southern Tunisia.

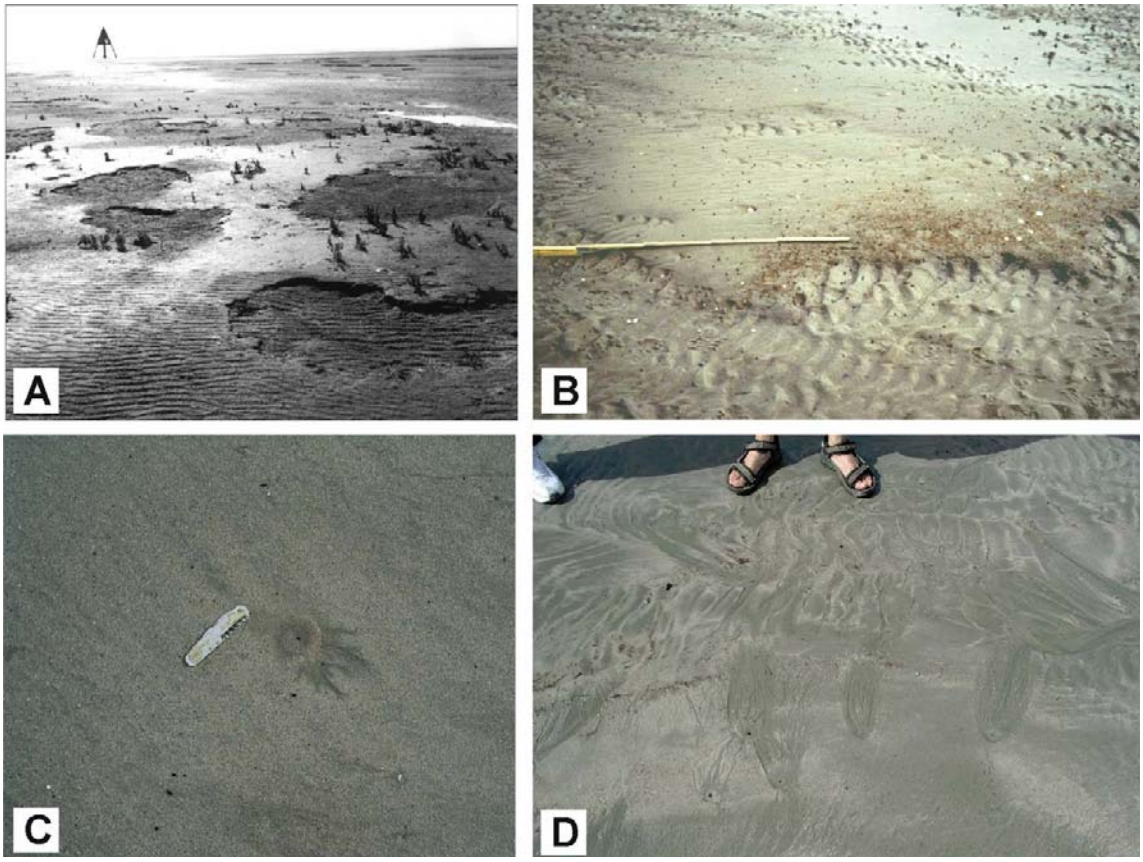

Figure 2-3-4. Ripple patches, "*Astropolithon*"-like features:

(A) Slightly rounded, rippled depressions of about 10 to 50 cm diameter on microbial mat-stabilized siliciclastic tidal flats. Photo: H.-E. Reineck; modified after photo published in Reineck, 1979).

(B) Transition from the non-eroded biostabilized surface into a ripple patch; ripple crests merge laterally with the non-eroded surface. Eroded worm tubes at the margins. Photo: Nora Noffke.

(C) Individual "*Astropolithon*"-like feature on the surface of an intertidal beach: flat bulge rising on top of beach sand, central vertical pipe and dykes radiating from the central pipe. Host sediments are medium-grained quartz-sandy beach sands bound by a thin biofilm (knife is 8 cm long). Photo: B. Petzelberger.

(D) Similar locality as that shown in (C), but slightly different morphology of a series of sand volcanos across a steeper part of the intertidal beach, showing radiating dykes closer together than in (C). Photo: B. Petzelberger.

Locality of photos: (A) to (B) Mellum Island, southern North Sea coast (Germany); (C) to (D) Jericoacoara beach, NE Brazil.

Figure 2-4-1. *In situ* carbonate precipitation in evaporite microbial sediments:

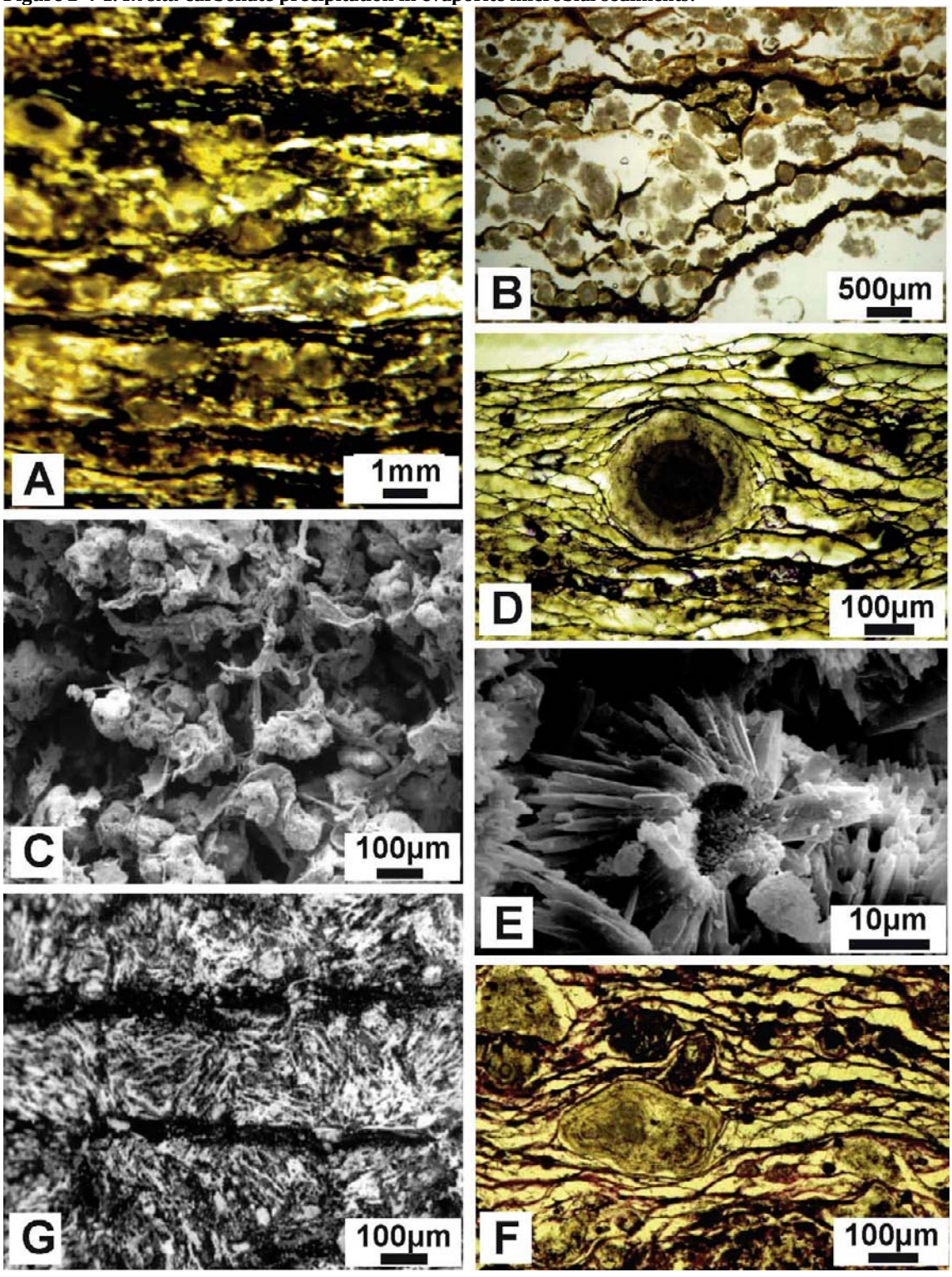

In: *Atlas of microbial mat features preserved within the clastic rock record*, Schieber, J., Bose, P.K., Eriksson, P.G., Banerjee, S., Sarkar, S., Altermann, W., and Catuneau, O., (Eds.), Elsevier, p. 5-38. (2007)

Figure 2-4-1. *In situ* carbonate precipitation in evaporite microbial sediments:

(A) Cross-section through growth-bedding (see Figure 2-1-2) containing lamina-specific arrangements of carbonate grains, biogeochemically formed *in situ*. Photo: Gisela Gerdes.

(B) Banded arrangement of granular carbonate inclusions in plastic microbial mats. Photo: Gisela Gerdes; modified after photo published in Gerdes et al. (2000b).

(C) SEM view of grape-like peloids attached to fragments of microbial mats. Photo: Gisela Gerdes; modified after photo published in Gerdes et al. (1994b).

(D) Section across cortoid-like particle showing opaque nucleus and translucent rim made of fibrous cement, organic matter scattered between aragonite crystals. Particle growth within elastic microbial meshwork gives rise to "sedimentary augen structure" (indications of compressed laminae at top and bottom of the particle and strained laminae to left and right). Photo: K. Dunajtschik-Piewak.

(E) SEM view of internal mat fabric showing hollow nucleus surrounded by radial aragonite. Photo: W.-E. Krumbein.

(F) Cross-section showing filamentous meshwork containing carbonate particles of various shapes and sizes. Centre: composite grain showing inclusions of microbial lumps or non-finished particles surrounded by a superficial coating, similar to botryoidal lumps. Photo: K. Dunajtschik-Piewak.

(G) Vertical section showing extended light laminae (summer generations, see Figure 2-1-2) interspersed with sheaths in diagonal to vertical orientation coated by calcium carbonate ("frozen" filaments). Photo: Gisela Gerdes; modified after photo published in Gerdes and Krumbein (1987).

Locality of photos: (A), (E) Solar Lake, Gulf of Aqaba coast (Egypt), hypersaline sea-marginal ecosystem; (B) to (D), (F) saltworks of Lanzarote, Canary Islands (Spain); (G) Gavish Sabkha, Gulf of Aqaba coast (Egypt), hypersaline sea-marginal ecosystem.

Figure 2-4-2. Fenestral fabrics:

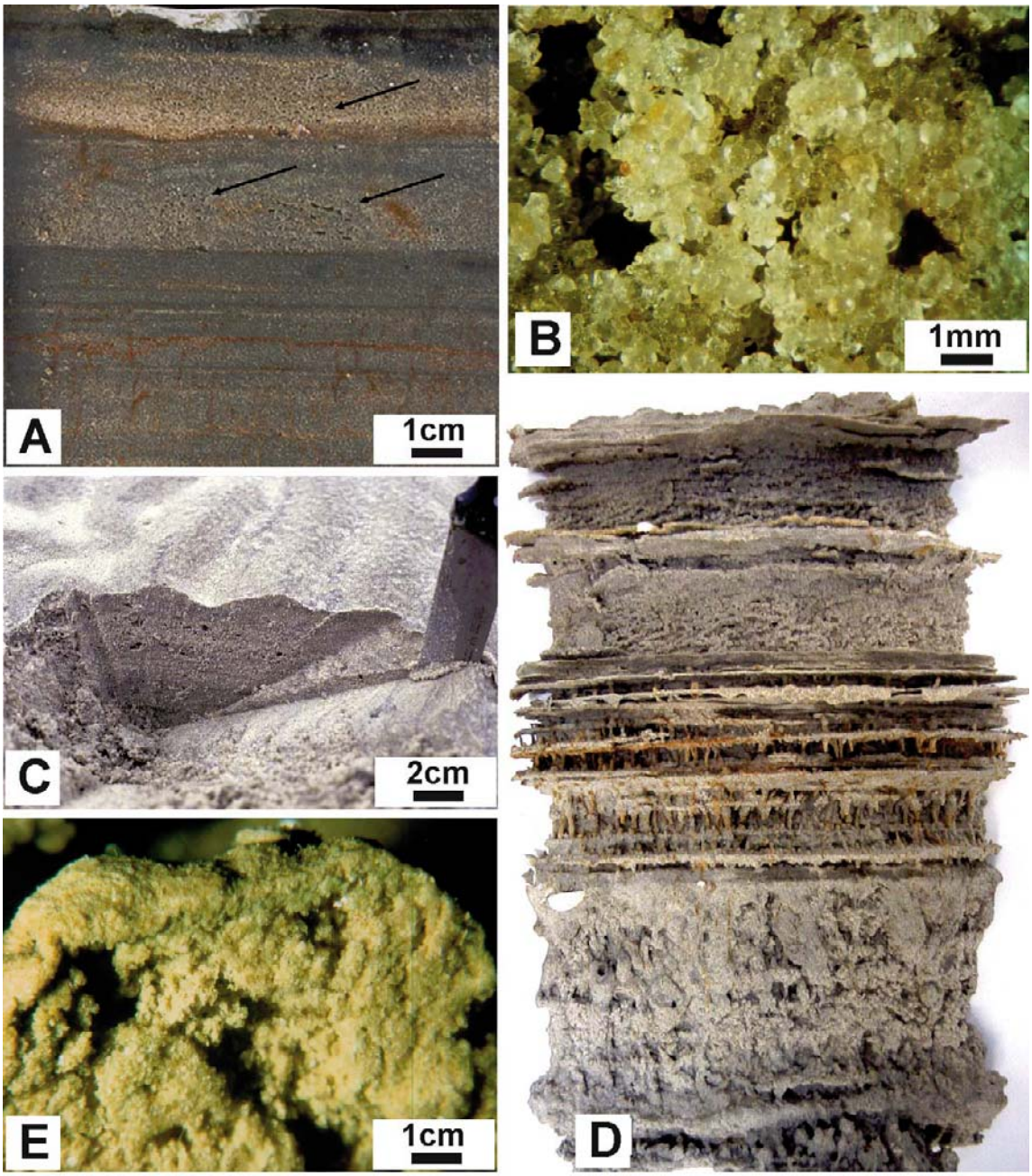

In: *Atlas of microbial mat features preserved within the clastic rock record*, Schieber, J., Bose, P.K., Eriksson, P.G., Banerjee, S., Sarkar, S., Altermann, W., and Catuneau, O., (Eds.), Elsevier, p. 5-38. (2007)

Figure 2-4-2. Fenestral fabrics:

A. Vertical section through biolaminites embedded in siliciclastic sediments. Arrows pointing to fenestral cavities caused by gas from the lower organic decay zone migrating towards the surface, captured by the sealing mats. Iron oxides mark sub-recent mats and root channels of salt marsh plants. Photo: Nora Noffke; modified after photo published in Gerdes et al. (2000a).

B. Close-up of quartz sands, secondary voids being produced by degassing of decaying organic material in the subground. Photo: Nora Noffke; modified after photo published in Gerdes et al. (2000a).

C. Oblique view and cross-section of rippled sand, elongated secondary pores caused by gas from lower organic decay zone and fixed by sealing mat layers. Photo: Nora Noffke.

D. Relief cast showing fenestral fabrics in the two topmost layers, each bordered by sharply projecting mats overprinting ripples (see slightly curved morphologies and cross-stratification in the layers underlying the mats). Middle part marked by growth-bedding penetrated by tubes of polychaetes and small amphibian crustaceans characteristic of higher-lying tidal flat areas (same as those visible in Figure 2-3-4 (B)). Lower part: strongly bioturbated intertidal sediments. Iron oxides confined to mats and worm tubes (organic influence). Relief = 30 cm thickness. Photo: H.-E. Reineck.

E. Cross-section of a gas dome forming in muddy sediments, gas from the lower organic decay zone producing large voids. Thin green mat on top. Photo: Nora Noffke.

Locality of photos: (A) to (D) Mellum Island, southern North Sea coast (Germany); (E) Bahar Alouane, southern Tunisia.

Figure 2-4-3. Gas domes:

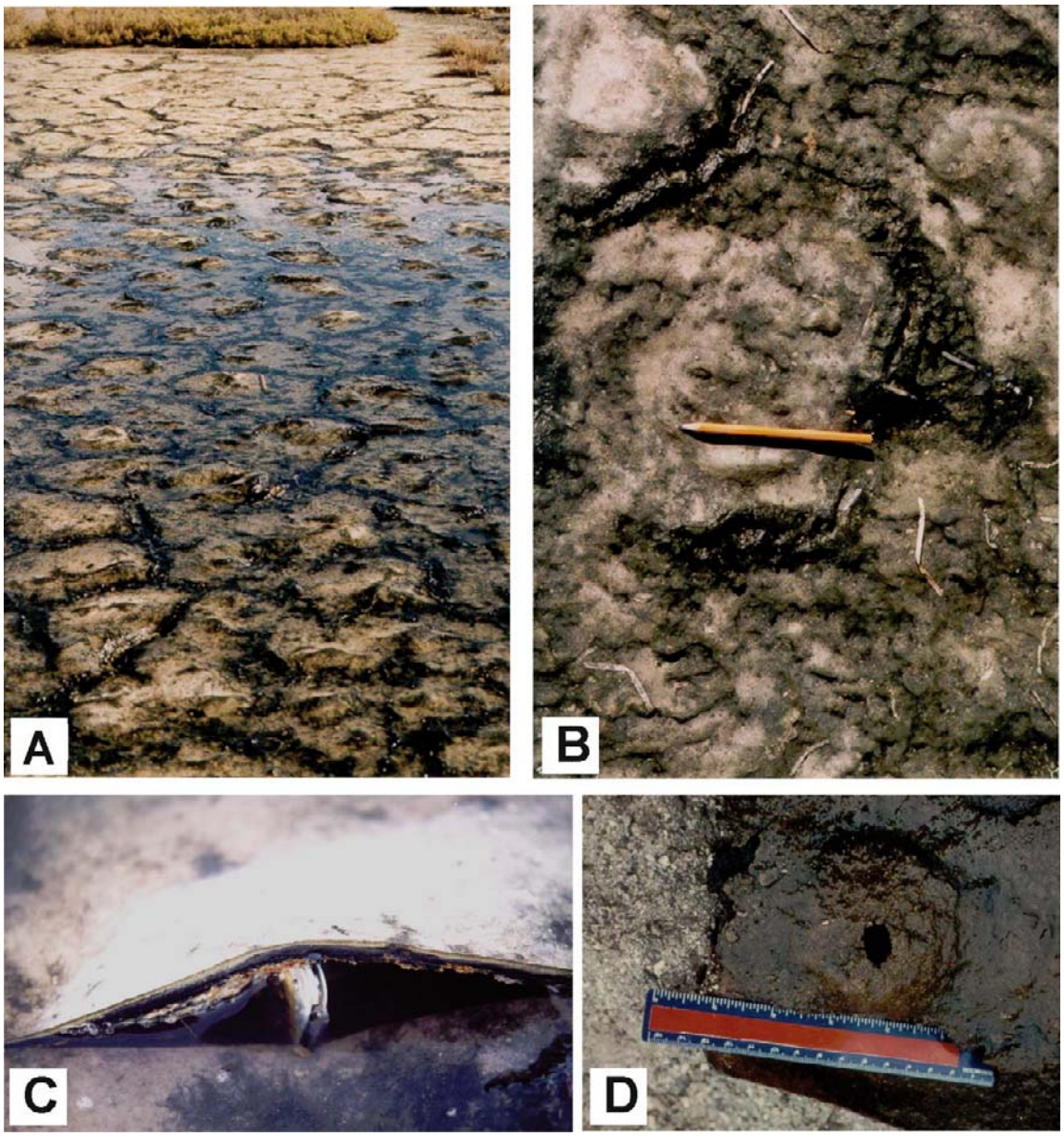

In: *Atlas of microbial mat features preserved within the clastic rock record*, Schieber, J., Bose, P.K., Eriksson, P.G., Banerjee, S., Sarkar, S., Altermann, W., and Catuneau, O., (Eds.), Elsevier, p. 5-38. (2007)

Figure 2-4-3. Gas domes:

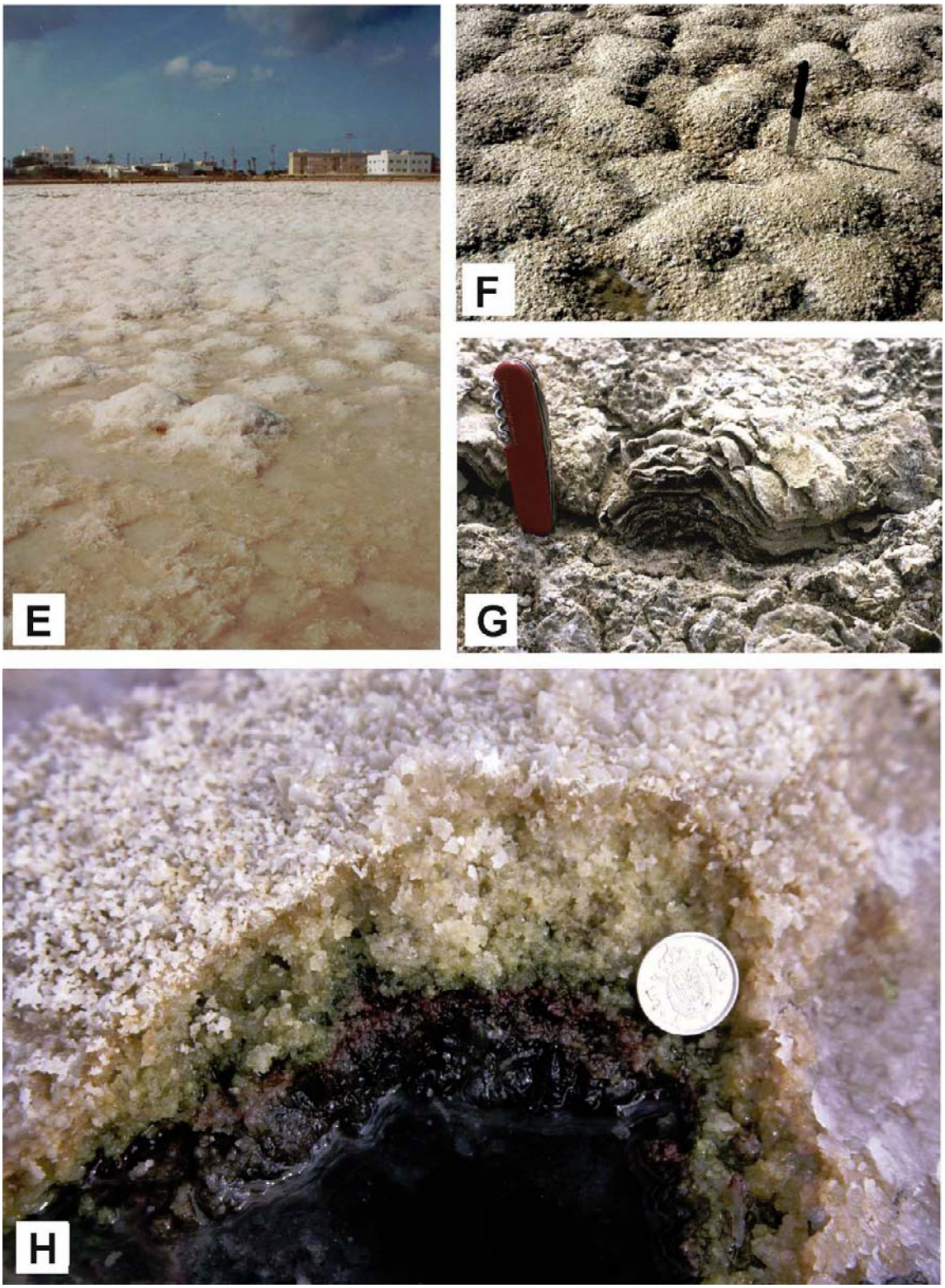

In: *Atlas of microbial mat features preserved within the clastic rock record*, Schieber, J., Bose, P.K., Eriksson, P.G., Banerjee, S., Sarkar, S., Altermann, W., and Catuneau, O., (Eds.), Elsevier, p. 5-38. (2007)

Figure 2-4-3. Gas domes:
(Figures showing bedding plane structures; ground planes about 30 cm in diameter).

(A) Gas domes in hypersaline shallow-water mats; yellow pencil for scale in middle of photograph. Photo: Nora Noffke; modified after photo published in Gerdes et al. (2000a).

(B) Soft-sediment dome partly collapsed, surrounding cracks re-colonized by microbial mats. Photo: Nora Noffke.

(C) Surface mat in shallow water artificially detached from the subground to show empty space below. Knife hindering collapse of the soft dome. Photo: Nora Noffke.

(D) Punctured gas dome. Gypsum crystals stabilizing the organic surface tissue prevented collapse. Photo: H.-E. Reineck; modified after photo published in Reineck et al. (1990).

(E) "Mole-hill"-like gas domes distributed on the bottom of a gypsum- and halite-encrusted salina basin. Photo: Gisela Gerdes.

(F) Closer view of evaporite-encrusted gas domes. Photo: H.-E. Reineck; modified after photo published in Gerdes et al., 1993.

(G) Typical cabbage-head structure within abandoned salina basin. Photo: H.-E. Reineck; modified after photo published in Gerdes et al., 1993.

(H) Salt-incrusted gas dome cut vertically to show the hollow centre. Reduced slushy ooze (black) forced in when the dome became opened (protuberance structures; Gerdes et al., 1993). Gypsum crust displaying colourful zonation of blue-green, purple phototrophs (dominant *Chromatium* sp.) and black sulphate-reducing zone. Photo: H.-E. Reineck.

Locality of photos: (A) to (B): Sabkha Amchoun, southern Tunisia; (C) Bahar Alouane, southern Tunisia; (D), (F) to (H) saltworks of Lanzarote, Canary Islands (Spain); (E) saltworks, Formentera, Balearic Islands (Spain);

Figure 2-4-4. Petee variations:

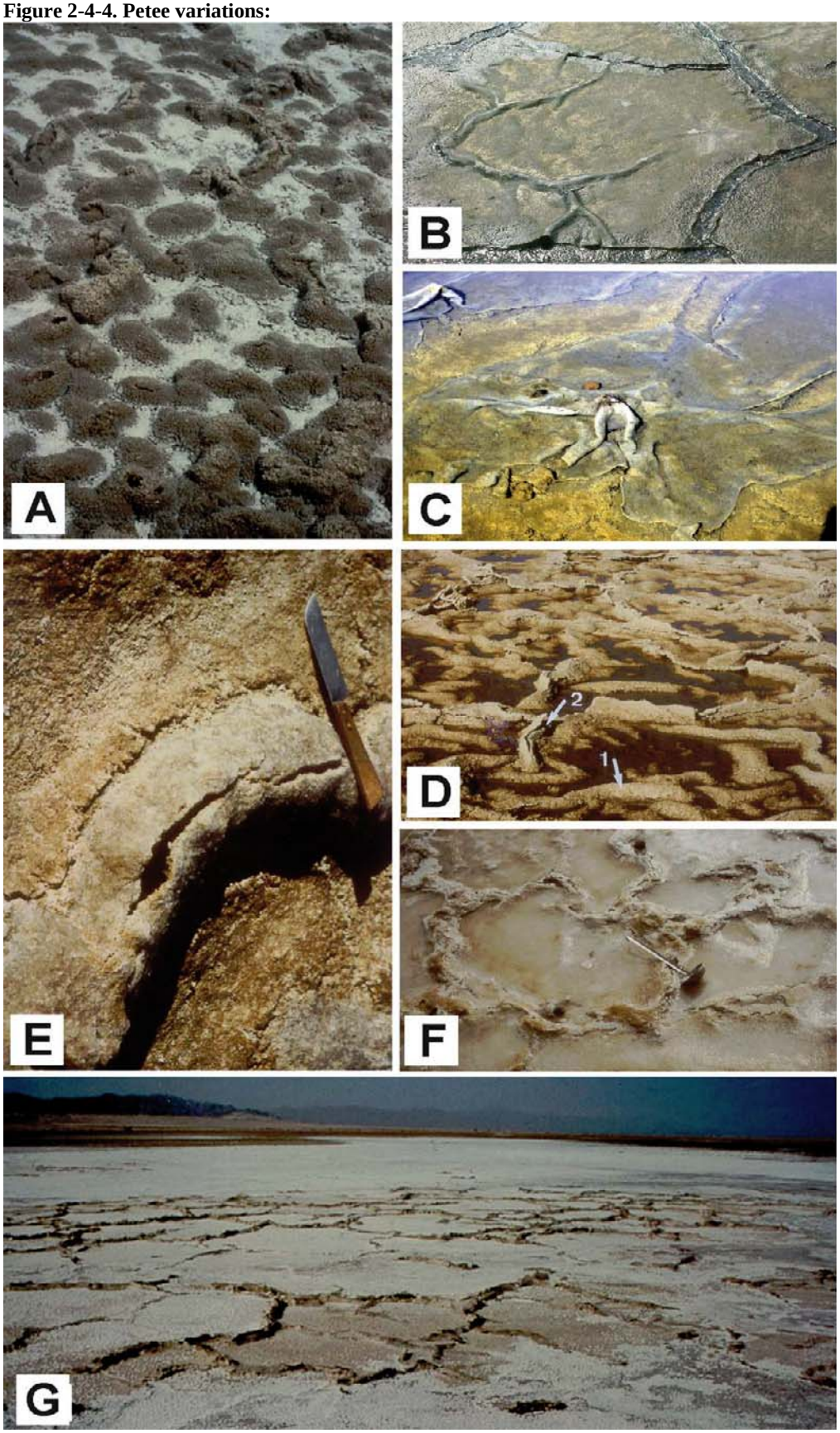

Figure 2-4-4. Petee variations:

In: *Atlas of microbial mat features preserved within the clastic rock record*, Schieber, J., Bose, P.K., Eriksson, P.G., Banerjee, S., Sarkar, S., Altermann, W., and Catuneau, O., (Eds.), Elsevier, p. 5-38. (2007)

(with reference to Reineck et al., 1990).

(A) Transitions from gas domes to elongated folds may be established by gas concentrated beyond the formerly non-encrusted, elastic and easily deformable mats. Photo: H.-E. Reineck; modified after photo published in Reineck et al. (1990).

(B) Monolayered soft microbial mat growing on a substrate enriched in clay minerals. Folding and tearing may be due to wind and/or water friction influencing the monolayered mat which shows low capacity to integrate into the subsoil (different to sandy sediments, see Figure 2-1-1 (C). Photo: J. Gifford; modified after photo published in Reineck et al. (1990).

(C) Similar monolayered soft microbial mat growing on a mixture of subaquatic gypsum and bacterial EPS. Mats scouring on the slippery substrate due to wind drift causing folds and tears. Wide tears and exposure of subsoil due to the non-sticking nature of the mat. Photo: H.-E. Reineck.

(D) Folds in initially elastic biogenic matrix of microbial mats subsequently gypsum-encrusted. Note rounded (1) and ruptured (2) crests. Photo: H.-E. Reineck; modified after photo published in Reineck et al. (1990).

(E) Close-up of elongated petee with ruptured crest. Rounded form of the crust, although ruptured, is initiated by elastic microbial mat. Photo: H.-E. Reineck; modified after photo published in Reineck et al. (1990).

(F) Polygonal overthrust structures in gypsum-encrusted microbial mats, crests ruptured (beta-petee). Photo: H.-E. Reineck; modified after photo published in Reineck et al. (1990).

(G) Polygonal overthrust structures in halite-encrusted terrigenous sabkha sediments (tepees and gamma petees. Polygon diameter increasing to 50 cm and more). Photo: W.-E. Krumbein; modified after photo published in Reineck et al. (1990).

Locality of photos: (A), (C) to (F) saltworks of Lanzarote, Canary Islands (Spain); (B) saltworks, Bretagne coast (France); (G) Gavish Sabkha, Gulf of Aqaba (Egypt), sea-marginal hypersaline ecosystem

References

Aigner, T., 1985. Storm depositional systems. In: S. Bhattacharya, G.M. Friedman, H.J. Neugebauer and A. Seilacher (Eds.) Lecture Notes in Earth Sciences, 3. Springer, Berlin, pp. 1-174.

Aitken, J.D., 1967. Classification and environmental significance of cryptalgal limestones and dolomites with illustrations from the Cambrian and Ordovician of Southwestern Alberta. J. Sediment. Petrol., 37: 1163-1178.

Assereto, R.L.A.M. and Kendall, C.G. St., 1977. Nature, origin and classification of peritidal tepee structures and related breccias. Sedimentology, 24: 153-210.

Astin, T.R. and Rogers, D.A., 1991. "Subaqueous shrinkage cracks" in the Devonian of Scotland reinterpreted. J. Sediment. Petrol., 61: 850-859.

Astin, T.R. and Rogers, D.A., 1993. "Subaqueous shrinkage cracks" in the Devonian of Scotland reinterpreted – reply. J. Sediment. Petrol., 63: 566-567.

Barclay, W.J., Glover, B.W. and Mendum, J.R., 1993. "Subaqueous shrinkage cracks" in the Devonian of Scotland reinterpreted – discussion. J. Sediment. Petrol., 63: 564-565.

Black, M., 1933. The algal sediments of Andros Island, Bahamas. Phil. Trns. Roy. Soc. London, B 222: 165-192.

Bouougri, E. and Porada, H., 2002. Mat-related sedimentary structures in Neoproterozoic peritidal passive margin deposits of the West African Craton (Anti-Atlas, Morocco). Sedimentary Geology, 153: 85-106.

Browne, K.M., Golubic, S. and Seong-Joo, L., 2000. Shallow marine microbial carbonate deposits. In: R.E. Riding and S.M. Awramik (Eds.) Microbial Sediments. Springer, Berlin, pp. 233-249.

Burne, R.V. and Moore, L.S., 1987. Benthic microbial communities and microbialites. In: Annual Report 1985. Baas Becking Geobiological Laboratory, pp. 10-12.

Castanier, S., Le Métayer-Levrel, G. and Perthuisot, J.-P., 2000. Bacterial roles in the precipitation of carbonate minerals. In: R.E. Riding and S.M. Awramik (Eds.) Microbial Sediments. Springer, Berlin, pp. 32-39.

Costerton, J. and Stoodley, P., 2003. Microbial biofilms: protective niches in ancient and modern geomicrobiology. In: W.E. Krumbein, D.M. Paterson and G.A. Zavarzin (Eds.) Fossil and Recent Biofilms. Kluwer, Dordrecht, pp. xv-xxi.

Dahanayake, K., Gerdes, G. and Krumbein, W.E., 1985. Stromatolites, oncolites and oolites biogenically formed in situ. Naturwissenschaften, 72: 513-518.

Dawson, J.W., 1878. Supplement to the 2nd edition of Acadian Geology. Acadian Geology, 3rd edition, Macmillan & Co, London, 102 p.

Demicco, R.V. and Hardie, L.A., 1994. Sedimentary structures and early diagenetic features of shallow marine carbonate deposits. SEPM Atlas Series, 1: 265 p.

Donovan, R.N. and Foster, R.J., 1972. Subaqueous shrinkage cracks from the Caithness Flagstone Series (Middle Devonian) of north east Scotland. J. Sediment. Petrol., 42: 309-317

Fagerstrom, J.A., 1967. Development, flotation, and transportation of mud crusts – neglected factors in sedimentology. J. Sediment. Petrol., 37: 73-79.

Fairbridge, R.W. and Bourgeois, J. (Eds.) (1978): The Encyclopedia of Sedimentology. Stroudsburg, Dowden, Hutchinson & Ross, Inc., 901 pp.

Fischer, A.G., 1964. The Lofer cyclothems of the Alpine Triassic. Kan. Geol. Survey Bull.. 169: 107-149.

Flügel, E., 2004. Microfacies of carbonate rocks. Springer, Berlin, 976 pp.

Friedman, G.M. and Krumbein, W.E. (Eds.), 1985. Hypersaline Ecosystems: The Gavish Sabkha. Springer, Berlin, 484 pp.

Friedman, G.M., Sanders, J.E. and Kopaska-Merkel, D., 1992. Principles of Sedimentary Deposits. MacMillan, New York.

Garcia-Pichel, F. and Castenholz, R.W., 1994. On the significance of solar ultraviolet radiation for the ecology of microbial mats. In: L.J. Stal and P. Caumette (Eds.) Microbial Mats: Structure, Development and Environmental Significance. Springer, Berlin, pp. 77-84.

Gavish, E., Krumbein, W.E. and Halevy, J., 1985. Geomorphology, mineralogy and groundwater geochemistry as factors of the hydrodynamic system of the Gavish Sabkha. In: G.M. Friedman and W.E. Krumbein (Eds): Hypersaline ecosystems: The Gavish Sabkha. Springer, Berlin, pp. 186-217.

Gehling, J.G., 1991. The case for Ediacaran fossil roots to the metazoan tree. Geol. Soc. India Memoir, 20: 181-224.

Gehling, J.G., 1999. Microbial mats in terminal Proterozoic siliciclastics: Ediacaran death masks. Palaios, 14: 40-57.

Gerdes, G. and Klenke, T., 2003. Geologische Bedeutung ökologischer Zeiträume in biogener Schichtung (Mikrobenmatten, potentielle Stromatolithe). Mitt. Ges. Geol. Bergbaustud. Österr., 46: 35-49.

Gerdes, G. and Krumbein, W.E., 1987. Biolaminated deposits. In: S. Bhattacharya, G.M. Friedman, H.J. Neugebauer and A. Seilacher (Eds.) Lecture Notes in Earth Sciences, 9. Springer, Berlin, pp. 1-183.

Gerdes, G., Krumbein, W.E. and Holtkamp, E.M., 1985. Salinity and water activity related zonation of microbial communities and potential stromatolites of the Gavish Sabkha. In: G.M. Friedman and W.E. Krumbein (Eds.) Hypersaline Ecosystems: The Gavish Sabkha. Springer, Berlin, pp. 238-266.

Gerdes, G., Krumbein, W.E. and Reineck, H.-E., 1991. Biolaminations – ecological versus depositional dynamics. In: G. Einsele, W. Ricken and A. Seilacher (Eds.) Cycles and Events in Stratigraphy. Springer, Berlin, pp. 592-607.

Gerdes, G., Claes, M., Dunajtschik-Piewak, K., Riege, H., Krumbein, W.E. and Reineck, H.-E., 1993. Contribution of microbial mats to sedimentary surface structures. Facies, 29: 61-74.

Gerdes, G., Krumbein, W.E. and Reineck, H.-E., 1994a. Microbial mats as architects of sedimentary surface structures. In: W.E. Krumbein, D.M. Paterson and L.J. Stal (Eds.) Biostabilization of sediments. BIS, Oldenburg, pp. 165-182.

Gerdes, G., Dunajtschik-Piewak, K., Riege, H., Taher, A.G., Krumbein, W.E. and Reineck, H.E., 1994b. Structural diversity of biogenic carbonate particles in microbial mats. Sedimentology, 41: 1273-1294.

Gerdes, G., Klenke, Th. and Noffke, N., 2000a: Microbial signatures in peritidal siliciclastic sediments, a Catalogue. Sedimentology, 47: 279-308.

Gerdes, G., Krumbein, W.E. and Noffke, N., 2000b. Evaporite microbial sediments. In: R.E. Riding and S.M. Awramik (Eds.) Microbial Sediments. Springer, Berlin, pp. 196-208.

Golubic, S., 1973. The relationship between blue-green algae and carbonate deposits. In: N.G. Carr and B.A. Whitton (Eds.) The Biology of Blue-green Algae. Blackwell, Oxford, pp. 434-472.

Golubic, S., 1976. Organisms that build stromatolites. In: M.R. Walter (Ed.) Stromatolites. Developments in Sedimentology 20. Elsevier, Amsterdam, pp. 113-126.

Golubic, S., 1992. Microbial mats of Abu Dhabi. In: L. Margulis and L. Olendzenski (Eds) Environmental evolution, effects of the origin and evolution of life on planet earth. MIT Press, Cambridge, pp. 131-147.

Hagadorn, J.W. and Bottjer, D.J., 1997. Wrinkle structures: Microbially mediated sedimentary structures common in subtidal siliciclastic settings at the Proterozoic-Phanerozoic transition. Geology, 25: 1047-1050.

Hagadorn, J.W. and Bottjer, D.J., 1999. Restriction of a Late Neoproterozoic biotope: suspect-microbial structures and trace fossils at the Vendian-Cambrian transition. Palaios, 14, 73-85.

Hofmann, H.J., 2000. Archean stromatolites as microbial archives. In: R.E. Riding and S.M. Awramik (Eds.) Microbial Sediments. Springer, Berlin, pp. 315-327.

Jorgensen, B.B., 1994. Diffusion processes and boundary layers in microbial mats. In: L.J. Stal and P. Caumette (Eds.) Microbial mats. Springer, Berlin, pp. 243-253

Krumbein, W.E., 1983. Stromatolites - the challenge of a term in space and time. Precambrian Res., 20: 493-531.

Krumbein, W.E., Buchholz, H., Franke, P., Giani, D., Giele, C. and Wonneberger, C., 1979. O_2 and H_2S coexistence in stromatolites. A model for the origin of mineralogical lamination in stromatolites and banded iron formations. Naturwissenschaften, 66: 381-389.

Krumbein, W.E., Brehm, U., Gorbushina, A.A., Levit, G. and Palinska, K.A., 2003 Biofilm, biodictyon and biomat – biolaminites, oolites, stromatolites – geophysiology, global mechanism and parahistology. In: W.E. Krumbein, D.M. Paterson and G.A. Zavarzin (Eds.) Fossil and Recent Biofilms. Kluwer, Dordrecht, pp. 1-27.

Kühl, M., Fenchel, T. and Kazmierczak, J., 2003. Growth, structure and calcification potential of an artificial cyanobacterial mat. In: W.E. Krumbein, D.M. Paterson and G.A. Zavarzin (Eds.) Fossil and Recent Biofilms. Kluwer, Dordrecht, pp. 77-102.

Logan, B.W., Hoffman, P. and Gebelein, C.D., 1974. Algal mats, cryptalgal fabrics, and structures, Hamelin Pool, Western Australia. In: B.W. Logan, P. Hoffman and C.D. Gebelein (Eds.) Evolution and Diagenesis of Quaternary Carbonate Sequence, Shark Bay, West Australia. AAPG Mem., 22, Tulsa, Oklahoma, pp. 140-194

Maia, L.P., 1998. Procesos Costeros y Balance Sedimentario a lo Largo de Fortaleza (NE Brazil): Implicationes para una Gestión Adecuada de la Zona litoral. PhD thesis, Faculty of Geology, University of Barcelona

Merz, M.U.E., 1992. The biology of carbonate precipitation by cyanobacteria. Facies, 26: 81-102.

Noffke, N., 1997. Mikrobiell induzierte Sedimentstrukturen (M.I.S.S) in siliziklastischen Wattablagerungen. Thesis, University of Oldenburg, 127 pp.

Noffke, N., 1998. Multidirected ripple marks rising from biological and sedimentological processes in modern lower supratidal deposits (Mellum Island, southern North Sea). Geology, 26: 879-882.

Noffke, N., 1999. Erosional remnants and pockets evolving from biotic-physical interactions in a Recent lower supratidal environment. Sediment. Geol., 123:175-181.

Noffke. N., 2000. Extensive microbial mats and their influences on the erosional and depositional dynamics of a siliciclastic cold water environment (Lower Arenigian, Montagne Noire, France). Sediment. Geol., 136: 207-215.

Noffke, N., Gerdes, G., Klenke, Th. and Krumbein, W.E., 1997a. A microscopic sedimentary succession indicating the presence of microbial mats in siliciclastic tidal flats. Sediment. Geol., 110: 1-6.

Noffke, N., Gerdes, G., Klenke, Th. and Krumbein, W.E., 1997b. Biofilm impact on sedimentary structures in siliciclastic tidal flats. Cour. Forsch.-Inst. Senckenberg, 201: 297-305.

Noffke, N., Gerdes, G., Klenke, T. and Krumbein, W.E., 2001. Microbially induced sedimentary structures – a new category within the classification of primary sedimentary structures. J. Sediment. Res., 71: 649-656.

Noffke, N., Knoll, A.H. and Grotzinger, J.P., 2002: Sedimentary controls on the formation and preservation of microbial mats in siliciclastic deposits: a case study from the Upper Neoproterozoic Nama Group, Namibia. Palaios, 17: 533-544.

Noffke, N., Gerdes, G. and Klenke, T., 2003a. Benthic cyanobacteria and their influence on the sedimentary dynamics of peritidal depositional systems (siliciclastic, evaporitic salty, and evaporitic carbonatic). Earth-Science Reviews, 62: 163-176.

Noffke, N., Hazen, R. and Nhleko, N., 2003b. Earth's earliest microbial mats in a siliciclastic marine environment (2.9 Ga Mozaan Group, South Africa). Geology, 31: 673-676.

Paterson, D.M., Yates, M.G., Wiltshire, K.H., McGrorty, S.M., Eastwood, A., Blackburn J. and Davidson, I., 1998. Microbiological mediation of spectral reflectance from intertidal cohesive sediments. Limnol. Oceanog., 43: 107-1221.

Paterson, D.M., Perkins, R., Consalvey, M. and Underwood, G.J.C., 2003. Ecosystem function, cell micro-cycling and the structure of transient biofilms. In: W.E. Krumbein, D.M. Paterson and G.A. Zavarzin (Eds.) Fossil and Recent Biofilms. Kluwer, Dordrecht, pp. 47-63.

Pflüger, F., 1999. Matground structures and redox facies. Palaios, 14: 25-39.

Reineck, H.-E., 1969. Die Entstehung von Runzelmarken. Natur Museum, 99: 386-388.

Reineck, H.-E., 1979. Rezente und fossile Algenmatten und Wurzelhorizonte. Natur Museum, 109: 290-296.

Reineck, H.-E. and Gerdes, G., 1997. Tempestites in Recent shelf and tidal environments of the southern North Sea. Cour. Forsch.-Inst. Senckenberg, 201: 361-370.

Reineck, H.-E. and Singh, I.B., 1980. Depositional Sedimentary Environments. 2nd ed. rev. updated. Springer, Berlin, 549 p.

Reineck, H.-E., Gerdes, G., Claes, M., Dunajtschik, K., Riege, H. and Krumbein, W.E., 1990. Microbial modification of sedimentary surface structures. In: D. Heling, P. Rothe, U. Förstner and P. Stoffers (Eds.) Sediments and Environmental Geochemistry. Springer, Berlin, pp. 254-276.

Sami, T.T. and James, N.P., 1993. Evolution of an early Paleozoic foreland basin carbonate platform, lower Pethei Group, Great Slave Lake, north-west Canada. Sedimentology, 40: 403-430.

Sarkar, S., Banerjee, S. and Eriksson, P.G., 2004. Microbial mat features in sandstones illustrated. In: P.G. Eriksson, W. Altermann, D.R. Nelson, W.U. Mueller and O. Catuneanu (Eds.) The Precambrian Earth: Tempos and Events. Developments in Precambrian Geology 12 (K.C. Condie, Series Editor), Elsevier, Amsterdam, pp. 673-675.

Schieber, J., 1998. Possible indicators of microbial mat deposits in shales and sandstones: Examples from the Mid-Proterozoic Belt Supergroup, Montana, USA. Sediment. Geol., 120: 105-124.

Schieber, J., 1999. Microbial mats in terrigenous clastics: the challenge of identification in the rock record. Palaios, 14: 3-12.

Schieber, J., 2004. Microbial mats in the siliciclastic rock record: a summary of diagnostic features. In: P.G. Eriksson, W. Altermann, D.R. Nelson, W.U. Mueller and O. Catuneanu (Eds.) The Precambrian Earth: Tempos and Events. Developments in Precambrian Geology 12 (K.C. Condie, Series Editor), Elsevier, Amsterdam, pp. 663-673

Schneider, J., 1995. Eindunstung von Meerwasser und Salzbildung in Salinen. Kali Steinsalz, 11: 325-330.

Schneider, J. and Herrmann, A.G., 1980. Saltworks – natural laboratories for microbiological and geochemical investigations during the evaporation of seawater. In: A.H. Coogan and L. Hauber (Eds.) V. Symposium on Salt, 2, Northern Ohio Geol. Soc., Inc., Ohio, pp. 371-381.

Schneider, J. and Le Campion-Alsumard, T., 1999. Construction and destruction of carbonates by marine and freshwater cyanobacteria. Eur. J. Phycol., 34: 417-426.

Seilacher, A. and Goldring, R., 1996. Class Psammocorallia (Coelenterata, Vendian-Ordovician): Recognition, systematics, and distribution. Geologiska Föreningens I Stockholm Förhandlingar, 118: 207-216.

Simonson, B.M. and Carney, K.E., 1999. Roll-up structures: evidence of in situ microbial mats in Late Archean deep shelf environments. Palaios, 14: 13-24.

Skyring, G.W., Lynch, R.M. and Smith, G.D., 1989. Quantitative relationships between carbon, hydrogen, and sulphur metabolism in cyanobacterial mats. In: Y. Cohen and E. Rosenberg (Eds.) Microbial mats, physiological ecology of benthic microbial communities. American Soc. Microbiol., Washington, D.C., pp.170-179

Stal, L.J., 1994. Microbial mats: ecophysiological interactions related to biogenic sediment stabilization. In: W.E. Krumbein, D.M. Paterson and L.J. Stal (Eds.) Biostabilization of Sediments. BIS Oldenburg, pp. 41-53.

Walter, M.R.D., 1976. Introduction. In: M.R. Walter (ed.) Stromatolites. Elsevier Publ. Co, Amsterdam, pp. 1-3.